

Gradual Domain Adaptation for Graph Learning

PUI IENG LEI, Faculty of Science and Technology, University of Macau, China

XIMING CHEN, Faculty of Science and Technology, University of Macau, China

YIJUN SHENG, Faculty of Science and Technology, University of Macau, China

YANYAN LIU, Faculty of Science and Technology, University of Macau, China

ZHIGUO GONG, Faculty of Science and Technology, University of Macau, China

QIANG YANG, PolyU Academy for Artificial Intelligence, Hong Kong Polytechnic University, China

Existing machine learning literature lacks graph-based domain adaptation techniques capable of handling large distribution shifts, primarily due to the difficulty in simulating a coherent evolutionary path from source to target graph. To meet this challenge, we present a *graph gradual domain adaptation* (GGDA) framework, which constructs a compact domain sequence that minimizes information loss during adaptation. Our approach starts with an efficient generation of knowledge-preserving intermediate graphs over the Fused Gromov-Wasserstein (FGW) metric. A GGDA domain sequence is then constructed upon this bridging data pool through a novel vertex-based progression, which involves selecting "close" vertices and performing adaptive domain advancement to enhance inter-domain transferability. Theoretically, our framework provides implementable upper and lower bounds for the intractable inter-domain Wasserstein distance, $W_p(\mu_t, \mu_{t+1})$, enabling its flexible adjustment for optimal domain formation. Extensive experiments across diverse transfer scenarios demonstrate the superior performance of our GGDA framework.

CCS Concepts: • **Theory of computation** → **Graph algorithms analysis**; • **Computing methodologies** → **Transfer learning**.

Additional Key Words and Phrases: Graph-Based Domain Adaptation, Gradual Domain Adaptation, Intermediate Domain Generation, Graph Neural Networks, Node Classification

ACM Reference Format:

Pui Ieng Lei, Ximing Chen, Yijun Sheng, Yanyan Liu, Zhiguo Gong, and Qiang Yang. 2025. Gradual Domain Adaptation for Graph Learning. *J. ACM* 37, 4, Article 111 (August 2025), 24 pages. <https://doi.org/XXXXXXXX.XXXXXXX>

1 INTRODUCTION

Domain adaptation (DA) provides a powerful framework for transferring knowledge from a label-rich source domain to a relevant but label-scarce target domain under data distribution shifts [41]. Traditionally, most DA algorithms rely on the assumption that data samples within each domain are independent and identically distributed (IID) [2, 8, 13, 32, 35, 36, 50, 55, 59, 71]. Recently, this assumption is increasingly challenged by the prevalence of non-IID data in real-world applications, such as social and traffic networks. Coupled with the rapid advancement of graph neural

Authors' addresses: Pui Ieng Lei, yc37460@um.edu.mo, Faculty of Science and Technology, University of Macau, Macau, China; Ximing Chen, Faculty of Science and Technology, University of Macau, Macau, China, yc37921@um.edu.mo; Yijun Sheng, Faculty of Science and Technology, University of Macau, Macau, China, yc17419@um.edu.mo; Yanyan Liu, Faculty of Science and Technology, University of Macau, Macau, China, yc07402@um.edu.mo; Zhiguo Gong, Faculty of Science and Technology, University of Macau, Macau, China, fstzgg@um.edu.mo; Qiang Yang, PolyU Academy for Artificial Intelligence, Hong Kong Polytechnic University, Hong Kong, China, profqiang.yang@polyu.edu.hk.

Permission to make digital or hard copies of all or part of this work for personal or classroom use is granted without fee provided that copies are not made or distributed for profit or commercial advantage and that copies bear this notice and the full citation on the first page. Copyrights for components of this work owned by others than the author(s) must be honored. Abstracting with credit is permitted. To copy otherwise, or republish, to post on servers or to redistribute to lists, requires prior specific permission and/or a fee. Request permissions from permissions@acm.org.

© 2025 Copyright held by the owner/author(s). Publication rights licensed to ACM.

Manuscript submitted to ACM

Manuscript submitted to ACM

networks (GNNs) [10, 15, 20, 27, 62, 74], this trend has spurred growing interest in DA for graph-structured data [3, 6, 24, 31, 33, 34, 38, 67–69, 79].

In graph DA, source and target graphs are defined not only by their data objects (nodes) but also by the relations between them (edges). Consequently, unlike in IID settings, data representations in graph DA must encode information from both individual nodes and their local neighborhoods. A standard approach involves learning a graph encoder that captures data dependencies via neighborhood aggregations while simultaneously aligning the source and target distributions in a latent space to facilitate transfer on a domain-invariant basis [9, 33, 44, 51, 68, 69, 78]. Nevertheless, theoretical analysis indicates that domain-invariant techniques often perform poorly under large marginal distribution shifts due to information distortion [82]. This problem is further amplified in non-IID graph scenarios, where node attributes and graph structure may shift jointly. Motivated by these challenges, our paper delves into the critical problem of graph domain adaptation under large distribution shifts. We adhere to an unsupervised domain adaptation (UDA) setting where the target domain is entirely unlabeled.

In IID-based UDA, to handle larger distribution shifts, several algorithms integrate the use of unlabeled intermediate domains between source and target domains [22, 40, 57, 75, 83]. A specific line of research investigates *gradual domain adaptation* (GDA), which leverages iterative model adaptations across a sequence of intermediate domains that transition gradually from source to target [1, 5, 21, 47, 56, 66]. Conceptually, GDA decomposes a single UDA problem with a large domain gap into a series of smaller ones with reduced gaps, thereby providing a tighter bound on the generalization error. While such intermediate sequences are occasionally available from data collection (e.g., portraits taken across years or evolving social networks), it is often difficult or impossible to obtain suitable intermediate data. To overcome this, IID methods generate virtual intermediate data through techniques like interpolation and adversarial training [1, 21, 40, 75].

Despite its promising performance, GDA has been confined to IID settings, and its applicability to complex non-IID data remains underexplored. Given the growing ubiquity of graph-structured data, it is critical to prevent the performance of graph DA models from plummeting under large shifts — a scenario where GDA is poised to be highly valuable. Motivated by this gap, we introduce and explore a novel *graph gradual domain adaptation* (GGDA) framework from theoretical and empirical perspectives. Assuming no intermediate data is initially available, our work addresses the central question: *In a non-IID context of graph-structured data, how can we construct an intermediate domain sequence to ensure high target accuracy in GGDA?*

To answer this, we first identify two key criteria: (1) the intermediate domains should be constructed to *minimize information loss* during adaptation, and (2) the construction scheme should allow for the *flexible adjustment* of the inter-domain Wasserstein distance, $W_p(\mu_t, \mu_{t+1})$, to optimize domain formation. In a graph context, this presents two primary challenges: (1) $W_p(\mu_t, \mu_{t+1})$ is inherently implicit due to the lack of an explicitly defined structure space for accommodating all possible instance relations, and (2) the generation of each instance must jointly account for both the node itself and its neighborhood structure.

Based on these considerations, we propose a novel GGDA framework. We first develop an efficient method to generate a sequence of intermediate graphs with weighted Fréchet mean over the Fused Gromov-Wasserstein (FGW) metric [58], a graph distance metric defined as the minimal cost of transporting both node features and structural relations between two graphs. In this way, we bypass the need to know the implicit cross-domain structures. Our proposed entropy-guided matching strategy, combined with coupling constraints in FGW computations, maximizes the infusion of valid and discriminative knowledge from the original graphs into the generated data. Upon this generated data bridge, we introduce a novel domain progression scheme to construct a sequence of GGDA domains with enhanced

inter-domain compactness, facilitating robust knowledge transfer. This scheme comprises two modules: (1) a regularized vertex selection process for constructing the subsequent domain, and (2) an adaptive mass decay mechanism for removing obsolete nodes from the current domain. By traversing the generated graphs and populating each domain with "close" vertices, the resulting cross-domain adaptation effectively preserves the most transferable and discriminative knowledge.

Theoretically, we demonstrate that the otherwise intractable $W_p(\mu_t, \mu_{t+1})$ is now concretized by its lower bound from the FGW metric and its upper bound from our vertex selection regularization. Furthermore, a hyperparameter governing the scale of vertex selection under our prioritization enables the flexible adjustment of $W_p(\mu_t, \mu_{t+1})$ to optimize domain formation without the need for expensive, repetitive data generation. Our key contributions are summarized as follows:

- To the best of our knowledge, we are the first to investigate *gradual domain adaptation on graphs* and propose a novel solution specifically tailored to overcome *large domain gaps* in non-IID graph DA tasks.
- Our GGDA framework constructs a compact domain sequence to enable stable knowledge transfer. We address the fundamental challenge of structural implicitness by designing tractable modules with provable bounding effects on the inter-domain distance.
- We conduct extensive experiments on fifteen benchmark datasets. The results consistently validate our theoretical insights and demonstrate the framework’s effectiveness, showing an average performance gain of +5.02% over the best baseline.

2 RELATED WORKS

This section provides a concise overview of prior research. A comprehensive discussion is available in the appendix.

2.1 Graph Domain Adaptation

The prevailing paradigm for node-level graph domain adaptation employs adversarial training to learn domain-invariant representations that can fool a domain discriminator [3, 6, 9, 19, 31, 33, 34, 38, 44, 51, 52, 67–70, 78, 79, 81]. Beyond adversarial alignment, alternative strategies have been explored, such as ego-graph information maximization [85], spectral regularization that modulates the GNN Lipschitz constant for error bounding [78], and generation of a new source graph [24]. Despite these advances, no existing approaches have addressed the critical scenario of large distribution gaps between source and target graphs. Graph-level domain adaptation, on the other hand, focuses on graph classifications and treats each graph as an individual sample, more closely resembling traditional IID settings [76, 77].

2.2 Intermediate Domains for IID Domain Adaptation

Leveraging intermediate domains has proven effective for IID domain adaptation [1, 5, 16, 18, 21, 22, 28, 40, 42, 57, 66, 75, 83]. Early approaches constructed these domains as subspaces on manifolds (e.g., Grassmann) [16, 18], while later works generate them at the sample level to better integrate with deep learning techniques [1, 17, 21, 40, 75]. A specific strategy, gradual domain adaptation (GDA), progressively adapts a source model to the target along a path of intermediate domains, which are either retrieved from data or generated via interpolation and mixup strategies [5, 21, 28, 47, 53, 56, 66]. Despite its success in IID settings, the potential of intermediate domains and GDA for non-IID graph data has not been investigated, leaving a critical gap in handling large graph distribution shifts.

2.3 Optimal Transport

The optimal transport (OT) framework provides a principled way to quantify the discrepancy between probability distributions by computing the minimal cost required to transport mass from one distribution to another. The Wasserstein distance was first proposed as a metric between distributions dwelling in a common metric space [25, 46], whereas the Gromov-Wasserstein (GW) distance was developed to be applied across different metric spaces by comparing their intrinsic relational structures [39, 42]. Fused Gromov-Wasserstein (FGW) distance was proposed recently as a combination of the two distances above [58, 61]. The OT framework has found versatile applications in graph learning, including graph clustering, graph partitioning, graph representation learning, etc. [4, 7, 30, 37, 43, 48, 58, 61, 63–65, 72, 73].

3 PRELIMINARIES

This section establishes our formal setting, including: (1) key mathematical notations, (2) definitions of graph space and domain distributions, and (3) specification of models and learning objectives in GGDA.

3.1 Notations

A simplex of n bins is denoted by $\Sigma_n = \{h \in \mathbb{R}_+^n \mid \sum_i h_i = 1\}$. For two histograms $h \in \Sigma_n$ and $h' \in \Sigma_m$, we denote the set of all couplings between h and h' by $\Pi(h, h') = \{\pi \in \mathbb{R}_+^{n \times m} \mid \sum_i \pi_{i,j} = h'_j; \sum_j \pi_{i,j} = h_i\}$. For a space Ω and $x \in \Omega$, δ_x denotes the Dirac measure in x . The support of probability measure $\mu \in P(\Omega)$ is denoted by $\text{supp}(\mu) = \text{argmin}_A \{|A| \mid A \subset \Omega; \mu(\Omega \setminus A) = 0\}$.

3.2 Graph Space

In this paper, a graph is viewed as a distribution sampled from a product space of features, structures, and classes. An undirected attributed graph $\mathcal{G} = (\mathcal{V}, \mathcal{E})$ contains the set of vertices \mathcal{V} and edges \mathcal{E} . Each vertex $v_i \in \mathcal{V}$ has (1) a feature representation x_i in space (Ω_x, d_x) , (2) a structure representation a_i in space (Ω_a, C) , and (3) a class label y_i in space (Ω_y, d_y) .

Specifically, the feature space Ω_x is a Euclidean space, with d_x being the Euclidean distance. For simplicity, we focus on binary classification in this paper, with node labels $y_i \in \{-1, 1\}$ and $\Omega_y := \mathbb{R}$. The structure space Ω_a is an implicit space, upon which the exact positions of nodes are not observed, and $C : \Omega_a \times \Omega_a \rightarrow \mathbb{R}_+$ measures the distance between pairs of nodes reflected by their structures in the graph, such as node adjacency or shortest path distance. Note that in graph DA setting, since relational semantics persist across domains (e.g., for citation networks from different time periods, edges always represent citation relationships), we assume a shared ground structure space (Ω_a, C) for all graphs. In other words, the structural distance between nodes from different graphs is well-defined by C , even if the corresponding inter-graph edges (e.g., potential citations between papers from different time periods) are unobserved.

For a graph with n vertices, a histogram $h \in \Sigma_n$ describes each vertex's relative importance within the graph (e.g., uniform or degree distribution). This allows the graph to be represented as $\mu = \sum_{i=1}^n h_i \delta_{(x_i, a_i, y_i)}$, a fully supported probability measure over the product space $\Omega_x \times \Omega_a \times \Omega_y$. Given that not all labels are observed, the graph can also be represented in a reduced product space $\Omega_x \times \Omega_a$, i.e., $\mu = \sum_{i=1}^n h_i \delta_{(x_i, a_i)}$.

In a graph domain adaptation setting, we view all graphs concerned to be drawn from a shared space $\Omega_x \times \Omega_a \times \Omega_y$, but with shifted probability distributions.

3.3 Models and Objectives

Consider a node classification task, where the goal is to predict node labels from node features and graph topology. Given a model family Θ , for each $\theta \in \Theta$, a model $M_\theta : \Omega_x \times \Omega_a \rightarrow \Omega_y$ outputs the classification predictions. Each model can be viewed as a composite function with respect to some Euclidean embedding space (Ω_z, d_z) , i.e., $M_\theta = \Psi_\theta \circ \Phi_\theta$, where $\Phi_\theta : \Omega_x \times \Omega_a \rightarrow \Omega_z$ (graph encoder) and $\Psi_\theta : \Omega_z \rightarrow \Omega_y$ (classifier).

Consider $T + 1$ graph distributions (i.e., domains), denoted by $\mu_0, \mu_1, \dots, \mu_T$. For unsupervised graph DA, $\mu_0 = \mu_S$ is a fully-labeled source domain and μ_T is a fully-unlabeled target domain. For GGDA, μ_1, \dots, μ_{T-1} are unknown intermediate domains transitioning from source to target. The population loss in t -th domain is defined as

$$\epsilon_t(\theta) \equiv \epsilon_{\mu_t}(\theta) = \mathbb{E}_{x,a,y \sim \mu_t} [\ell(M_\theta(x, a), y)], \quad (1)$$

where ℓ is the loss function. The goal is to find a model M_θ that yields a low classification error on the target graph, i.e., low $\epsilon_T(\theta)$.

4 ASSUMPTIONS

Our framework is built upon the following assumptions.

Assumption 1. (Covariate shift) Assume the conditional distribution $p(y|x, a)$ is invariant over the ground space [54].

Assumption 2. (Metrics on product spaces) Assume the metric on $(\Omega_x \times \Omega_a, d_{(x,a)})$ is a linear combination of the metrics on the respective space, i.e., $d_{(x,a)}((x, a), (x', a')) = (1 - \alpha)d_x(x, x') + \alpha C(a, a')$ for some $\alpha \in [0, 1]$. Meanwhile, assume the metric on $(\Omega_x \times \Omega_a \times \Omega_y, d_{(x,a,y)})$ is the Manhattan distance along the input and output coordinates, i.e., $\Omega_x \times \Omega_a$ and Ω_y .

Assumption 3. (Bounded model complexity) Given a graph domain where the number of training samples is n and the maximum degree is d_{max} , assume the Rademacher complexity of the considered GNN model family Φ is bounded by [14]:

$$\mathfrak{R}_n(\Phi) \leq O\left(\frac{d_{max}}{\sqrt{n}}\right). \quad (2)$$

Assumption 4. (Lipschitz model) Assume for any $\theta \in \Theta$, the model M_θ is R -Lipschitz in the implicit input space $(\Omega_x \times \Omega_a, d_{(x,a)})$ for some $R > 0$, and the model Ψ_θ is \tilde{R} -Lipschitz in the Euclidean embedding space (Ω_z, d_z) for some $\tilde{R} > 0$:

$$\begin{aligned} |M_\theta((x, a)) - M_\theta((x', a'))| &\leq R \cdot d_{(x,a)}((x, a), (x', a')), & \forall (x, a), (x', a') \in \Omega_x \times \Omega_a; \\ |\Psi_\theta(z) - \Psi_\theta(z')| &\leq \tilde{R} \cdot d_z(z, z'), & \forall z, z' \in \Omega_z. \end{aligned} \quad (3)$$

Assumption 5. (Lipschitz loss) Assume the loss function ℓ is ρ -Lipschitz in the output space Ω_y for some $\rho > 0$ [66]:

$$\begin{aligned} |\ell(y, \cdot) - \ell(y', \cdot)| &\leq \rho |y - y'|, \\ |\ell(\cdot, y) - \ell(\cdot, y')| &\leq \rho |y - y'|, & \forall y, y' \in \Omega_y. \end{aligned} \quad (4)$$

5 ANALYSIS OF GGDA DOMAIN GENERATION

Our goal is to transfer knowledge between the relevant source and target graphs under a large distribution shift. In the absence of naturally occurring intermediate data, we aim to generate a sequence of intermediate domains that

promotes stable long-range knowledge transfer. Formal proofs of the generalization bound and all propositions in this paper are provided in the appendix.

Our primary consideration is to establish the criteria that intermediate domains should satisfy to guarantee a well-bounded target error for GGDA. Following previous GDA work [66], we adopt an online learning perspective and obtain the following generalization bound for graph-based gradual domain adaptation:

$$\epsilon_T(\theta_T) \leq \epsilon_0(\theta_0) + \mathcal{O}\left(T\Delta + T\left(e + \sqrt{\frac{\log(1/\delta')}{b}}\right)\right) + \tilde{\mathcal{O}}\left(\frac{1}{\sqrt{nT}}\right),$$

$$\text{where } \Delta = \frac{1}{T} \sum_{t=0}^{T-1} W_p(\mu_t, \mu_{t+1}) \text{ and } \mu_t = \sum_{i=1}^{n_t} h_i^t \delta_{(x_i^t, a_i^t, y_i^t)}.$$
(5)

Here n indicates the average number of vertices in each domain. The terms e and $\sqrt{\frac{\log(1/\delta')}{b}}$ quantify the inherent non-IID nature of the given dataset and are beyond the scope of our optimization. Our analysis focuses on the critical term Δ , defined as the average p-Wasserstein distance (i.e., W_p) between consecutive domains. This metric captures the combined disparity in features, structures, and labels across domains under an optimal coupling. We observe an inverse relationship between the optimal Δ and T [66], suggesting that when the average distance between consecutive domains is large, the number of intermediate domains should be fewer, and vice versa. Note that this does not imply that the bound is tightest at $T = 1$ (i.e., non-GDA). In fact, both Eq. (5) and past empirical GDA studies [28, 66] indicate that optimal performance is typically achieved at a "sweet spot" when T is moderately large (i.e., Δ is moderately small). This further underscores the necessity of a graph GDA algorithm that strategically decomposes a large shift into a sequence of manageable, smaller transitions to enhance overall adaptation performance.

Based on this analysis, we identify two criteria for successful intermediate domain generation in GGDA: (1) the length of the path connecting source and target, i.e., $T\Delta$, should be small to curb information loss during transfer, and (2) the search for the optimal Δ should be conducted under an inverse relationship between Δ and T . Fulfilling these criteria presents three key challenges:

- (1) Both criteria require generating domains based on the inter-domain distance $W_p(\mu_t, \mu_{t+1})$ over $\Omega_x \times \Omega_a \times \Omega_y$. This is highly non-trivial since (i) $W_p(\mu_t, \mu_{t+1})$ over the structural space Ω_a is inherently implicit, and (ii) during generation, each created sample (i.e., vertex) within domain μ must be characterized by both its own attributes and its relational information with neighbors.
- (2) For criterion (1), an ideal solution is to generate a Wasserstein geodesic over $\Omega_x \times \Omega_a \times \Omega_y$, yet this is extremely challenging in practice due to the intractable optimization for an exact Wasserstein geodesic of attributed topological data.
- (3) While the p-Wasserstein metric is defined on $\Omega_x \times \Omega_a \times \Omega_y$, only the source domain is labeled. How the intermediate domains should be generated to effectively integrate class information (i.e., y -dimension) poses another key challenge.

To tackle challenge (1), we propose to facilitate domain generation by concretizing the graph metric (especially over the implicit topology on Ω_a) using the FGW distance, which acts as a bridge between the abstract distance W_p and practical implementations. Regarding challenge (2), we reformulate the goal of finding a geodesic into a tractable objective: *minimizing information loss during the GGDA process*. Specifically, we aim to approximate the shortest path between source and target by generating intermediate domains that minimize information loss upon model adaptations. This is achieved by a combination of FGW optimizations and a subsequent vertex selection process

for domain constructions. Additionally, the regularized vertex selection addresses challenge (3) through enhanced pseudo-labeling for domain progression. In the following sections, we will provide the detailed explanations accordingly.

6 GRAPH GENERATION OVER FGW METRIC

While we wish to generate intermediate domains based on the distance defined in Eq. (5), a primary challenge is the intractability of $W_p(\mu_t, \mu_{t+1})$ over the product space $\Omega_x \times \Omega_a \times \Omega_y$, which arises because the metric for measuring structural distance between samples from different graphs Ω_a is implicit (i.e., no inter-graph edges). This presents a dilemma specific to a non-IID context, where each sample is characterized not only by itself but also by its relationships with other attributed samples. To bridge this gap between theory and practice, we require a well-defined and tractable inter-graph distribution distance that jointly accounts for features and structures. To this end, we adopt the Fused Gromov-Wasserstein (FGW) distance, defined as follows.

Definition 1. (FGW distance) Let two attributed graphs be $\mu = \sum_{i=1}^n h_i \delta_{(x_i, a_i)}$ and $\nu = \sum_{j=1}^m h'_j \delta_{(x'_j, a'_j)}$. Let $d_x(i, j) = d_x(x_i, x'_j)$ be the distance between cross-network features, while $C(i, k) = C(a_i, a_k)$ and $C'(j, l) = C(a'_j, a'_l)$ are the respective structure matrix for μ and ν . Given the set of all admissible couplings $\Pi(h, h')$ and $\alpha \in [0, 1]$, the FGW distance in the discrete case is defined as [58]

$$FGW_{\alpha, p, q}(\mu, \nu) = \left(\min_{\pi \in \Pi(h, h')} E_{\alpha, p, q}(\pi) \right)^{\frac{1}{p}}, \quad \text{where} \quad (6)$$

$$E_{\alpha, p, q}(\pi) = \sum_{i, j, k, l} \left[(1 - \alpha) d_x(i, j)^q + \alpha |C(i, k) - C'(j, l)|^q \right]^p \pi_{i, j} \pi_{k, l}.$$

$E(\pi)$ represents the cost of transporting mass between graphs under a node matching strategy π . This cost combines the expense of transporting features across single nodes and transporting structures across pairs of nodes. The FGW distance is the minimal cost given by the optimal coupling. Hence, the computation of FGW is built upon sample coupling that preserves both feature and relation similarities. Under this formulation, node i is matched to node j only if they exhibit similar features and their respective neighbors (i.e., k, l) also present a correspondence.

6.1 Fast Entropy-Guided Graph Generation

Having established a tractable graph metric, we now generate intermediate graphs to bridge the source and target. Note that these "intermediate graphs" form a data pool from which "intermediate domains" will later be constructed. We propose to generate a sequence of $K - 1$ intermediate graphs $\{\tilde{\mu}_k\}_{k=1}^{K-1}$ by computing the weighted Fréchet mean [61] over the FGW metric on $\Omega_x \times \Omega_a$ (without Ω_y as μ_T is unlabeled). However, directly computing the Fréchet mean between the *entire* source and target graphs is computationally expensive for large graphs. To improve efficiency and preserve knowledge, we introduce a partition-based, entropy-guided graph generation strategy, where each intermediate graph $\tilde{\mu}_k$ is generated as a combination of smaller subgraphs $\{\tilde{\mu}_{k_i}\}_i$.

We first transform the source and target graphs into P_S and P_T partitions with METIS [26], an algorithm that minimizes edge cuts. The core idea is to generate each subgraph $\tilde{\mu}_{k_i}$ from a matched pair of source and target partitions, denoted by $\hat{\mu}_{m(P_t)}^S$ and $\hat{\mu}_{P_t}^T$, with indices $m(P_t) \in \{1, 2, \dots, P_S\}$ and $P_t \in \{1, 2, \dots, P_T\}$. The function $m(\cdot)$ represents an index matching between source and target partitions, which we aim to optimize to enhance knowledge preservation during graph generation.

We begin with a warm-up phase to obtain a preliminary matching $\dot{m}(\cdot)$. Let $m(\cdot)$ be a random matching, $n_{m(P_t)}^S$ and $n_{P_t}^T$ be the size of the partition pair, $Y_{m(P_t),c}^S \in \{0, 1\}^{n_{m(P_t)}^S}$ be an indicator of source nodes belonging to class $c \in \{-1, 1\}$, and $\pi^*(m(P_t), P_t) \in [0, 1]^{n_{m(P_t)}^S \times n_{P_t}^T}$ be the normalized FGW optimal coupling on $\Omega_x \times \Omega_a$ between the partition pair. Then, for each $P_t \in \{1, 2, \dots, P_T\}$, we compute the following:

$$\begin{aligned} f_{(m(P_t), P_t), c} &= \left[\text{diag}(Y_{m(P_t),c}^S) \cdot \pi^*(m(P_t), P_t) \right]^T \cdot \mathbf{1}, \\ F_{(m(P_t), P_t)} &= \left[f_{(m(P_t), P_t), -1}, f_{(m(P_t), P_t), 1} \right], \\ H_{(m(P_t), P_t)} &= \frac{1}{n_{P_t}^T} \sum_{i=1}^{n_{P_t}^T} \left[- \sum_j F_{(m(P_t), P_t), ij} \cdot \log F_{(m(P_t), P_t), ij} \right]. \end{aligned} \quad (7)$$

Here $F_{(m(P_t), P_t)} \in [0, 1]^{n_{P_t}^T \times 2}$ represents the push-forward class distribution for each target node, and $H_{(m(P_t), P_t)} \in \mathbb{R}$ is the average target node class entropy. While this distribution is estimated, it serves as a useful indicator of information compatibility between the pair $(m(P_t), P_t)$: a large H indicates that much valid class information has been lost by coupling this pair over FGW. Combining the effects of source class entropy H^S and FGW distance, for each pair $(m(P_t), P_t)$, we derive a measure of information loss

$$S_{\text{loss}}(m(P_t), P_t) = \left(H_{(m(P_t), P_t)} / H_{m(P_t)}^S \right) \cdot \text{FGW}(\hat{\mu}_{m(P_t)}^S, \hat{\mu}_{P_t}^T), \quad (8)$$

where all components are normalized. During the warm-up phase, different initializations of $m(\cdot) \in \mathcal{M}(\cdot)$ are employed, and a preliminary matching is set to $\dot{m}(P_t) = \operatorname{argmin}_{m(P_t) \in \mathcal{M}(P_t)} S_{\text{loss}}(m(P_t), P_t)$.

We now proceed to the knowledge-preserving graph generation using the matched partition pairs. In this phase, $m(P_t)$ is set to $\dot{m}(P_t)$ with a probability $\propto 1/S_{\text{loss}}(\dot{m}(P_t), P_t)$ and is set to a new matching otherwise. This strategy prioritizes low-loss matches while allowing for further optimization. Using this matching, we generate a sequence of unlabeled intermediate graphs $\{\tilde{\mu}_k\}_{k=1}^{K-1}$ over $\Omega_x \times \Omega_a$ via the following weighted Fréchet mean optimization for each k :

$$\begin{aligned} \tilde{\mu}_k &= \frac{1}{\Gamma} \sum_i \tilde{\mu}_{k_i}, \text{ where} \\ \tilde{\mu}_{k_i} &= \operatorname{argmin}_{\mu} \left[\left(\frac{K-k}{K} \right) \cdot \text{FGW}(\mu, \hat{\mu}_{m(P_{t,i})}^S) + \left(\frac{k}{K} \right) \cdot \text{FGW}(\mu, \hat{\mu}_{P_{t,i}}^T) \right], \end{aligned} \quad (9)$$

with $P_{t,i} \sim \text{Uniform}\{1, 2, \dots, P_T\}$ and Γ being a normalizing factor. This scheme constructs a bridging graph sequence $\{\tilde{\mu}_k\}_{k=1}^{K-1}$ by incrementally shifting the position of $\tilde{\mu}_k$ between μ_S and μ_T over the FGW metric. The index matching $\dot{m}(\cdot)$ is continuously refined when a new matching yields a smaller S_{loss} than the previous one. In this phase, $S_{\text{loss}}(m(P_t), P_t)$ is computed by substituting (1) the source-intermediate optimal coupling $\pi^*(m(P_{t,i}), k_i)$ in Eq. (7) and (2) the distance sum $\text{FGW}(\hat{\mu}_{m(P_{t,i})}^S, \tilde{\mu}_{k_i}) + \text{FGW}(\tilde{\mu}_{k_i}, \hat{\mu}_{P_{t,i}}^T)$ in Eq. (8). Both quantities are obtained directly as byproducts of the Fréchet mean optimization, requiring no additional computation. Since the entropy now reflects information loss relative to the intermediate graph $\tilde{\mu}_{k_i}$, the information integrity of the generated graphs is actively enhanced. Overall, our accelerated module largely reduces the time complexity of graph generation from $\mathcal{O}(n^3)$ to $\mathcal{O}(Pn_p^3)$, where P is the average number of partitions and n_p is the average partition size (see complexity analysis).

6.2 Analysis: Why Is FGW-Based Graph Generation Important for a Successful GGDA?

While the FGW-generated graphs do not directly conform to $W_p(\mu_t, \mu_{t+1})$ over $\Omega_x \times \Omega_a \times \Omega_y$ in Eq. (5), this proposed generation process is central to our algorithm for two reasons.

First, the minimization in Eq. (9) serves as a mechanism for information preservation in the construction of intermediate graphs by aiming to reduce the FGW distance between $\tilde{\mu}_{k_t}$ and $\hat{\mu}_S/\hat{\mu}_T$. The sample correspondence constraint inherent in FGW optimization forces the ego-graphs distributed in the generated $\tilde{\mu}_k$ to meaningfully interpolate and preserve the characteristics of source and target ego-graphs. In other words, this approach serves to *minimize the information loss* over $\Omega_x \times \Omega_a$ when generating the bridging data sequence.

Second, as discussed in Section 5, generating domains requires optimizing the intractable $W_p(\mu_t, \mu_{t+1})$ over $\Omega_x \times \Omega_a \times \Omega_y$. While this exact W_p distance is unattainable, it is, in fact, lower bounded by the FGW distance over $\Omega_x \times \Omega_a$, as formalized below.

Proposition 2. For graph measures $\mu(x, a, y) = \sum_{i=1}^n h_i \delta_{(x_i, a_i, y_i)}$ and $v(x', a', y') = \sum_{j=1}^m h'_j \delta_{(x'_j, a'_j, y'_j)}$, along with their marginal measures $\mu(x, a) = \sum_{i=1}^n h_i \delta_{(x_i, a_i)}$ and $v(x', a') = \sum_{j=1}^m h'_j \delta_{(x'_j, a'_j)}$,

$$W_p(\mu(x, a, y), v(x', a', y')) \geq FGW_{\alpha, p, 1}(\mu(x, a), v(x', a'))/2. \quad (10)$$

This relation implies that, to generate data with a certain W_p distance, a necessary condition is to reduce the FGW distance between the data. Intuitively, our FGW-based graph generation is a crucial first step for creating a bridging data pool that can subsequently be refined to achieve the desired $W_p(\mu_t, \mu_{t+1})$ and, ultimately, a successful GGDA process.

7 GGDA DOMAIN SEQUENCE CONSTRUCTION

Gradual domain adaptation (GDA) involves model training on a sequence of T domains with labeled data, such that the model shifts from source domain μ_0 to target domain μ_T with small steps over the intermediate domains $\{\mu_t\}_{t=1}^{T-1}$. Specifically, since only the source domain contains ground-truth labels, each intermediate domain is defined with pseudo-labels obtained during iterative training. To perform GDA on graphs, one major consideration, as discussed above, is how to properly define the intermediate domain sequence over $\Omega_x \times \Omega_a \times \Omega_y$ to minimize information loss during the GGDA process. Specifically, it is crucial to ensure that pseudo-labeling can be performed accurately when defining each labeled intermediate domain under our algorithm, thereby curbing the accumulation of label error and preserving transferable knowledge in GGDA.

7.1 Analysis: Vertex-Based Domain Construction for GGDA

Given the FGW-generated graph sequence, one might define each *intermediate domain* μ_t directly as a single *intermediate graph* $\tilde{\mu}_k|_{k=t}$ with post-assigned pseudo-labels. However, such a definition is suboptimal because the FGW distance itself is not an upper bound of $|\epsilon_{k+1}(\theta) - \epsilon_k(\theta)|$, i.e., it does not inherently guarantee information transferability (and thus the correctness of pseudo-labeling) from $\tilde{\mu}_k$ to $\tilde{\mu}_{k+1}$. To this end, we propose to construct each domain μ_t progressively during training by selecting vertices from the generated data pool. This strategy offers two key advantages, as described below.

First, the ultimate objective of GGDA is vertex-based node classification, which depends on the characteristics encoded in each vertex's ego-graph. Therefore, instead of treating an entire FGW-generated graph as an individual domain, defining each subsequent domain as a set of vertices selected based on their knowledge relevance to the previous domain better preserves the transferable and discriminative knowledge during adaptation. As presented in

Figure 1, we start with the labeled domain $\mu_S = \mu_0$ in training. Since vertices in the graph sequence vary in their relevance to μ_0 in terms of the $d_{(x,a,y)}$ metric (i.e., distance over $\Omega_x \times \Omega_a \times \Omega_y$), selecting vertices that are close to μ_0 (marked with "+") to form the subsequent domain μ_1 can better enhance cross-domain knowledge transfer by minimizing information loss.

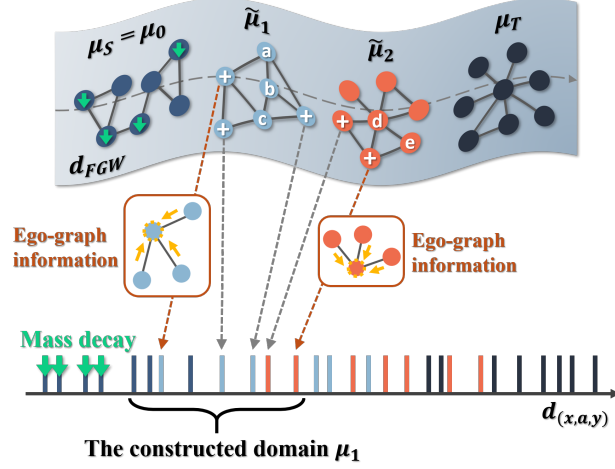


Fig. 1. Illustration of our GGDA framework's design rationale. The upper part shows the sequence of intermediate graphs generated in the FGW metric space, and the lower part shows the corresponding vertex relations over product space distance $d_{(x,a,y)}$. μ_0 (in dark blue) is initially labeled. For forming the subsequent domain μ_1 , vertices marked "+" are newly selected, while those with a green downward arrow are downweighted.

Second, since the newly constructed domain can incorporate vertices from different generated graphs, the domain's connections to unused vertices in the pool are naturally maintained through existing edges. Knowledge propagation across these edges improves the accuracy of pseudo-labeling on connected vertices, thereby elevating the quality of the next constructed domain. Put differently, the presence of inter-domain edges is the key to a successful GGDA, as it indicates greater transfer potential and reduced information loss between consecutive domains. In Figure 1, for example, if vertices marked with "+" are correctly pseudo-labeled and included in domain μ_1 , then vertices a to e , being prospective components of domain μ_2 , can receive accurate pseudo-labels via message passing from their reliably labeled neighbors. This insight regarding the importance of inter-domain connectivity is further supported theoretically, as shown in the following proposition.

Proposition 3. Consider graph domains $\mu = \sum_{i=1}^n h_i \delta_{(x_i, a_i, y_i)}$ and $\nu = \sum_{j=1}^m h'_j \delta_{(x'_j, a'_j, y'_j)}$ with uniform weights h and h' . Let \mathcal{E} be the set of unit-weight edges linking μ and ν and $\tilde{\pi}$ be an arbitrary coupling satisfying $\tilde{\pi}_{i,j} = \frac{1}{nm} \mathbb{1}_{\{(i,j) \in \mathcal{E}\}}$.

For any $\theta \in \Theta$, the population loss on μ and ν given by M_θ satisfies

$$\begin{aligned} |\epsilon_\mu(\theta) - \epsilon_\nu(\theta)| &\leq \rho(\zeta_1 + \zeta_2), \quad \text{where} \\ \zeta_1 &= \frac{\sqrt{\tilde{R}^2 + 1}}{n \cdot m} \sum_{(i,j) \in \mathcal{E}} \left(\|z_i(\theta) - z'_j(\theta)\| + |y_i - y'_j| \right), \\ \zeta_2 &= \sqrt{R^2 + 1} \cdot \left[\min_{\tilde{\pi}} \left(\sum_{(i,j) \notin \mathcal{E}} d_{(x,a,y)} \left((x_i, a_i, y_i), (x'_j, a'_j, y'_j) \right)^p \cdot \tilde{\pi}_{i,j} \right) \right]^{\frac{1}{p}}. \end{aligned} \quad (11)$$

When transferring a model between arbitrary graph domains μ and ν , the error bound consists of two components (i.e., ζ_1 and ζ_2) corresponding to node pairs *with* and *without* inter-domain edges, respectively. For ζ_1 , $\sum_{(i,j) \in \mathcal{E}} \|z_i(\theta) - z'_j(\theta)\|$ is small as most GNNs act as graph Laplacian regularizers that enforce similarity between the learned embeddings of two connected nodes [84]. Meanwhile, $\sum_{(i,j) \in \mathcal{E}} |y_i - y'_j|$ is small if the graphs are homophilic. For ζ_2 , however, the distance $\sum_{(i,j) \notin \mathcal{E}} d_{(x,a,y)}^p$ can be unbounded. We therefore expect a tighter bound when consecutive domains are well-connected (i.e., not mutually isolated), as this maximizes the contribution of the constrained ζ_1 term and minimizes the influence of the potentially large ζ_2 term.

7.2 The Domain Progression Framework

Motivated by the preceding analysis, we propose a GGDA framework that constructs the domain sequence $\{\mu_t\}_{t=0}^T$ progressively in a vertex-based manner during training. Specifically, given the current domain, we construct the subsequent domain with two novel modules: regularized vertex selection and adaptive mass decay.

Let $|M_\theta(x, a)|$ be the geometric margin and $\text{sign}(M_\theta(x, a))$ be the prediction, respectively. We treat the entire generated graph sequence as a single batched graph μ_B over $\Omega_x \times \Omega_a$, where $\mathcal{V}_B := \text{supp}(\mu_B) = \bigcup_{k=1}^{K-1} \text{supp}(\tilde{\mu}_k) \cup \text{supp}(\mu_S) \cup \text{supp}(\mu_T)$, and we initialize a mass decay mask $w_{v_b}^0 = 1$ for all $v_b \in \mathcal{V}_B$. Initially, only nodes from the source graph are labeled, so we define $\mu_0 = \mu_S = \sum_{i=1}^{n_S} h_i^S \delta_{(x_i^S, a_i^S, y_i^S)}$ with $h_i^S = 1/n_S$. In each iteration, we apply the following two modules to construct the subsequent domain μ_{t+1} and adapt the model from μ_t to μ_{t+1} .¹

7.2.1 Vertex Selection for Constructing the Next Domain. Let $\mathcal{V}_t^t := \text{supp}(\mu_t)$ denote the set of vertices of the current domain μ_t and $\mathcal{V}_u^t := \mathcal{V}_B \setminus (\bigcup_{t'=0}^t \mathcal{V}_t^{t'})$ be the set of unused vertices in the data pool. First, we train a new model θ_t on the current domain μ_t with the loss $\mathbb{E}_{x,a,\hat{y} \sim \mu_t} [\ell(M_{\theta_t}(x, a), \hat{y})] = \sum_{v_l \in \mathcal{V}_t^t} h_l^t \cdot \ell(M_{\theta_t}(x_l, a_l), \hat{y}_l)$, where \hat{y} is either a pseudo-label or a ground-truth label. In the inference phase, for each $v_u \in \mathcal{V}_u^t$, we compute a regularized score

$$\begin{aligned} c_u^t &= |M_{\theta_t}(x_u, a_u)| \cdot \exp\left(-\frac{d_u^t}{\max_{\{v_{u'} \in \mathcal{V}_u^t\}} d_{u'}^t} \cdot \eta\right), \\ \text{where } d_u^t &= \min_{v_l \in \mathcal{V}_t^t} d_z(\Phi_{\theta_t}(x_u, a_u), \Phi_{\theta_t}(x_l, a_l)). \end{aligned} \quad (12)$$

Here d_z is the Euclidean distance. In this module, we first obtain the node embeddings by aggregating the feature and structure information of each vertex encoded in its ego-graph, which is either given or generated over the FGW metric. An η -penalty mechanism then prioritizes vertices with high classification confidence within the embedding neighborhood of μ_t . Specifically, vertices are sorted by c_u^t and selected subject to a constraint κ , the ratio of new pseudo-label count per class to source label count per class. The selected vertex set, denoted by \mathcal{V}_{pl}^t , is incorporated into the next domain μ_{t+1} , with pseudo-labels $\hat{y}_{pl} = \text{sign}(M_{\theta_t}(x_{pl}, a_{pl}))$ for $v_{pl} \in \mathcal{V}_{pl}^t$. We assign sharpened pseudo-labels

¹From here till the end of section 7.2, we denote $(x_{v_s}, a_{v_s}, \hat{y}_{v_s}, h_{v_s}, w_{v_s})$ by $(x_s, a_s, \hat{y}_s, h_s, w_s)$.

(i.e., -1 or 1) rather than probabilities to encourage more decisive model updates [28]. To justify the design of this module, we present the following proposition.

Proposition 4. Let $\Phi_{\tilde{\theta}} : \Omega_x \times \Omega_a \rightarrow \Omega_z$ be an (L, γ) -quasiisometric graph embedding [12]. Let $\mu(z|\tilde{\theta}) = \sum_{i=1}^n h_i \delta_{z_i|\tilde{\theta}}$, $v(z'|\tilde{\theta}) = \sum_{j=1}^m h'_j \delta_{z'_j|\tilde{\theta}}$, and $\pi^* = \operatorname{argmin}_{\pi \in \Pi(h, h')} \sum_{i,j} d_z(z_i|\tilde{\theta}, z'_j|\tilde{\theta})^p \pi_{i,j}$. Then we have

$$W_p(\mu(x, a, y), v(x', a', y')) \leq \xi \text{ and } |\epsilon_\mu(\theta) - \epsilon_v(\theta)| \cdot \mathcal{O}(\rho^{-1}) \leq \xi, \quad (13)$$

$$\text{where } \xi = L \left[W_\infty(\mu(z|\tilde{\theta}), v(z'|\tilde{\theta})) + \gamma + \frac{1}{L} \left(\sum_{i,j} |y_i - y'_j|^p \pi_{i,j}^* \right)^{\frac{1}{p}} \right].$$

Proposition 4 leads to two key conclusions that validate our approach: (1) Under the covariate shift assumption, our vertex selection strategy based on the sorted score c_u^t adheres to ξ formulation by prioritizing samples that are within the Ω_z neighborhood and distant from the decision boundary. Therefore, modifying the hyperparameter κ , which controls the scale of class-proportionate vertex selection under c_u^t -prioritization, enables flexible adjustment of the inter-domain distance $W_p(\mu_t, \mu_{t+1})$ over $\Omega_x \times \Omega_a \times \Omega_y$ via its upper bound ξ while satisfying an inverse relationship between Δ and T . This provides a tractable mechanism to realize an efficient global search for the optimal GGDA domain path without requiring any repetitive data generation. (2) Meanwhile, since our proposed prioritization favors the selection of vertices close to μ_t over the metric $d_{(x,a,y)}$ for inclusion in the next domain μ_{t+1} , it ensures *minimal information loss* by preserving the most transferable and discriminative knowledge from μ_t to μ_{t+1} . Accordingly, a bounding effect on the local generalization error $|\epsilon_{t+1}(\theta) - \epsilon_t(\theta)|$ can be established to secure stable knowledge transfer upon the domain sequence.

7.2.2 Adaptive Mass Decay of Vertices. Due to the stochasticity in selecting \mathcal{V}_{pl}^t , strictly excluding all vertices \mathcal{V}_l^t from \mathcal{V}_l^{t+1} may result in low inter-domain connectivity in the succeeding iteration, degrading pseudo-label quality. Moreover, since a new model is trained in every domain, significantly more generated data is required if each domain contains only new vertices, which is inefficient. To this end, we propose an adaptive mass decay mechanism for the vertices in \mathcal{V}_l^t . Let the set of labeled nodes be $\mathcal{V}_{pll}^t := \mathcal{V}_l^t \cup \mathcal{V}_{pl}^t$. In every iteration, we store the label score $\hat{c}_{pll}^t = \hat{y}_{pll} \cdot M_{\theta_t}(x_{pll}, a_{pll})$ for $v_{pll} \in \mathcal{V}_{pll}^t$. Then, if $t \geq 1$, we compute the mass decay for $v_l \in \mathcal{V}_l^t$ as

$$\lambda_l^t = \exp\left(-\left[1 - \min\left(\frac{\hat{y}_l \cdot M_{\theta_t}(x_l, a_l)}{\hat{c}_l^{t-1}}, 1\right)\right] \cdot \beta\right). \quad (14)$$

This computation identifies the model flow after training in a new domain by quantifying the degradation in label correctness. Nodes with degraded labels will be downweighted in the next constructed domain to promote model advancement, with the hyperparameter β controlling the mass decay rate. We update the mask $w_l^t = w_l^{t-1} \cdot \lambda_l^t$ for $v_l \in \mathcal{V}_l^t$ cumulatively and define the next domain distribution as

$$\begin{aligned} \mu_{t+1} &= \frac{1}{\Gamma} \left(\sum_{v_l \in \mathcal{V}_l^t} w_l^t \cdot \delta_{(x_l, a_l, \hat{y}_l)} + \sum_{v_{pl} \in \mathcal{V}_{pl}^t} \delta_{(x_{pl}, a_{pl}, \hat{y}_{pl})} \right) \\ &= \sum_{v_{pll} \in \mathcal{V}_{pll}^t} h_{pll}^{t+1} \cdot \delta_{(x_{pll}, a_{pll}, \hat{y}_{pll})}, \end{aligned} \quad (15)$$

where Γ is a normalizing factor ensuring $\sum h_{pll}^{t+1} = 1$. In practice, we can keep only the top- k weighted samples in $\operatorname{supp}(\mu_{t+1})$ and assign a mass of 0 to others, where k is the average size of source and target graphs. The decay technique

is conceptually illustrated in Figure 1, with a minor distinction that this technique takes effect only when $t \geq 1$ (i.e., starting from the construction of μ_2). Note that while some target vertices might be labeled prior to the final stage, mass decay is not applied to these vertices, as our goal is to adapt to the target distribution. The GGDA process concludes with a final training step once a sufficient number of target vertices are confidently labeled.

8 COMPLEXITY ANALYSIS

For the generation of intermediate graphs, let P be the average number of partitions and $n_p \ll \max(n_S, n_T)$ be the average partition size. Then, the METIS partitioning takes $\mathcal{O}(Pn_p + (Pn_p)^2 + P \log(P)) = \mathcal{O}((Pn_p)^2)$, the warmup phase takes $\mathcal{O}(Pn_p^3)$, and the weighted Fréchet mean generation takes $\mathcal{O}(KPI n_p^3)$, with I denoting the number of iterations for block coordinate descent (BCD) [61]. Without loss of generality, the overall complexity for the generation phase in GGDA is $\mathcal{O}(KPI n_p^3)$. For comparison, generating intermediate graphs without partitioning would escalate the complexity to $\mathcal{O}(KIn^3)$, where n is the average size of source and target graphs, making the computation prohibitively expensive for large networks.

For the domain progression framework, the time complexity of model training in each domain is $\mathcal{O}(h|A_t^+|d^2)$, where h is the number of hops for GNN aggregations, d is the latent dimension, and $|A_t^+|$ is the number of edges in the subgraph induced by the set of labeled vertices in the current domain (i.e., $\mathcal{V}_t^t := \text{supp}(\mu_t)$) and their h -hop neighborhoods. The time complexity of each subsequent domain construction is $\mathcal{O}(|\mathcal{V}_t^t| |\mathcal{V}_u^t| d^2)$, where $|\mathcal{V}_u^t|$ is the number of samples in the data pool that have not been labeled before.

9 ALGORITHM

The algorithm of our proposed GGDA framework is shown in Algorithm 1.

10 EXPERIMENTS

Our goal is to examine whether the proposed GGDA framework improves graph knowledge transfer through its constructed domain sequence. We focus on cross-network node classifications, where source labels are used for training and target labels are used for validation and testing under a 2:8 ratio [33]. We conduct transfer experiments on fifteen graph datasets. Additional experiments, implementation details, and elaborations of datasets and baseline methods are provided in the appendix.

10.1 Datasets

Table 1 shows the statistics of the datasets. For datasets within the following four groups, we use one as source and the other as target.

- **ACM** (pre-2008), **Citation** (post-2010), and **DBLP** (2004 to 2008) (denoted by **A**, **C**, **D**): multi-label citation networks extracted from ArnetMiner [51];
- **ACM2** (2000 to 2010) and **DBLP2** (post-2010), (denoted by **A2**, **D2**): another pre-processed version of single-label citation networks [69];
- **Blog1** and **Blog2** (denoted by **B1**, **B2**): social networks from BlogCatalog, with 30% of the binary attributes randomly flipped to enlarge discrepancy [29];
- **Arxiv 2007, 2016, 2018**: Arxiv computer science citation networks partitioned by time (all from year 1950) [23].

Algorithm 1 The Proposed GGDA Framework.

Input: labeled source graph μ_S , unlabeled target graph μ_T , number of partitions P_S and P_T , number of intermediate graphs $K - 1$, tolerance of unlabeled ratio in target graph r_u^T , score penalty η , selection ratio κ , mass decay β

Output: node classification predictions on target graph

- 1: Partition μ_S and μ_T into P_S and P_T subgraphs by METIS.
- 2: **for** $P_t \in \{1, 2, \dots, P_T\}$ **do**
- 3: **for** $m(P_t) \in \mathcal{M}(P_t)$ **do**
- 4: Compute the information loss $S_{loss}(m(P_t), P_t)$ by Eq. (7) and (8).
- 5: **end for**
- 6: Set the preliminary matching to $\dot{m}(P_t) = \operatorname{argmin}_{m(P_t) \in \mathcal{M}(P_t)} S_{loss}(m(P_t), P_t)$.
- 7: **end for**
- 8: **for** $k = 1 : (K - 1)$ **do**
- 9: For $P_t \in \{1, 2, \dots, P_T\}$, set $m(P_t)$ to $\dot{m}(P_t)$ with a probability $\propto 1/S_{loss}(\dot{m}(P_t), P_t)$, and set it to a new matching otherwise.
- 10: Generate intermediate graph $\tilde{\mu}_k$ over the FGW metric by Eq. (9).
- 11: Using results from graph generation, compute $S_{loss}(m(P_t), P_t)$ by refined Eq. (7) and (8) w.r.t. intermediate graph entropy.
- 12: Update the matching $\dot{m}(P_t) = m(P_t)$ if $S_{loss}(m(P_t), P_t) < S_{loss}(\dot{m}(P_t), P_t)$.
- 13: **end for**
- 14: Define μ_B as the graph sequence, i.e., $\mathcal{V}_B := \operatorname{supp}(\mu_B) = \bigcup_{k=1}^{K-1} \operatorname{supp}(\tilde{\mu}_k) \cup \operatorname{supp}(\mu_S) \cup \operatorname{supp}(\mu_T)$.
- 15: Initialize mass decay mask $w_b^0 = 1$ for all $v_b \in \mathcal{V}_B$.
- 16: Initialize the first domain $\mu_0 = \mu_S$.
- 17: Initialize $t = 0$.
- 18: **while** $1 - |\operatorname{supp}(\mu_t) \cap \operatorname{supp}(\mu_T)| / |\operatorname{supp}(\mu_T)| \leq r_u^T$ **do**
- 19: Define $\mathcal{V}_l^t := \operatorname{supp}(\mu_t)$; $\mathcal{V}_u^t := \mathcal{V}_B \setminus (\bigcup_{l'=0}^t \mathcal{V}_l^{l'})$.
- 20: Initialize and train θ_t on μ_t with loss $\mathbb{E}_{x,a,\hat{y} \sim \mu_t} [\ell(M_{\theta_t}(x, a), \hat{y})]$.
- 21: Compute the regularized score c_u^t for $v_u \in \mathcal{V}_u^t$ using Eq. (12).
- 22: Sort $v_u \in \mathcal{V}_u^t$ by c_u^t and choose top-scored ones within constraint κ as \mathcal{V}_{pl}^t . Assign pseudo-labels $\hat{y}_{pl} = \operatorname{sign}(M_{\theta_t}(x_{pl}, a_{pl}))$ for $v_{pl} \in \mathcal{V}_{pl}^t$.
- 23: Define $\mathcal{V}_{pll}^t := \mathcal{V}_l^t \cup \mathcal{V}_{pl}^t$.
- 24: Store the label score $\hat{c}_{pll}^t = \hat{y}_{pll} \cdot M_{\theta_t}(x_{pll}, a_{pll})$ for $v_{pll} \in \mathcal{V}_{pll}^t$.
- 25: **if** $t \geq 1$ **then**
- 26: Compute the mass decay λ_l^t for $v_l \in \mathcal{V}_l^t$ using Eq. (14).
- 27: Update the mask $w_l^t = w_l^{t-1} \cdot \lambda_l^t$ for $v_l \in \mathcal{V}_l^t$.
- 28: **end if**
- 29: Define the next domain distribution μ_{t+1} using Eq. (15).
- 30: Set $t = t + 1$.
- 31: **end while**
- 32: Apply M_{θ_t} on μ_T to obtain classification predictions.

For citation networks **Cora** and **CiteSeer** [49], as well as Twitch social networks **ENGB**, **DE**, and **PTBR** [45], we simulate a *multi-step shifting process* independently on each graph to mimic gradual data shifts. Specifically, we perform 5 steps of class-wise feature shifts generated with Gaussian noise. This effectively shifts the distribution in $\Omega_x \times \Omega_a$ since both $p(x)$ and $p(a|x)$ have changed accordingly. These datasets with multi-step shifting will be used for evaluation in different ways, as detailed later.

Table 1. Statistics of datasets.

Graph	# Nodes	# Edges	Density	# Features	# Classes
ACM	9360	15602	0.0004	6775	5
Citation	8935	15113	0.0004	6775	5
DBLP	5484	8130	0.0005	6775	5
ACM2	7410	11023	0.0004	7537	6
DBLP2	5578	7290	0.0005	7537	6
Blog1	2300	33471	0.0127	8189	6
Blog2	2896	53836	0.0128	8189	6
Arxiv 2007	4980	5849	0.0005	128	40
Arxiv 2016	69499	232419	0.0001	128	40
Arxiv 2018	120740	615415	0.0001	128	40
Cora	2708	5278	0.0014	1433	7
CiteSeer	3327	4552	0.0008	3703	6
ENGB	7126	35324	0.0014	3170	2
DE	9498	153138	0.0034	3170	2
PTBR	1912	31299	0.0171	3170	2

10.2 Baselines

We compare our GGDA framework with the following baselines: **CDAN** [35], **MDD** [80], **UDA-GCN** [69], **ACDNE** [51], **ASN** [79], **GRADE** [68], **StruRW** [33], **SpecReg** [78], **GraphAlign** [24], **A2GNN** [31], **Pair-Align** [34], and **TDSS** [6]. Specifically, CDAN and MDD are non-graph DA methods, for which we replace the encoder with GCN [27]. All other baselines are graph DA methods under the **domain-invariant representation (DIR)** framework, except for GraphAlign, which is the first data-centric graph DA method introduced recently. While multiple baselines incorporate advanced encoder designs to enhance transfer performance, for our **GGDA** framework, we focus on three fundamental encoders in this paper: **GCN**, **GAT**, and **GraphSAGE** [20, 27, 62]. Additionally, we include two baselines trained with ground-truth information. **GGDA-GT** performs GGDA on the ground-truth intermediate graphs from the *multi-step shifting process*, while **Oracle** is trained on a labeled target graph.

10.3 Main Results

Table 2, Table 3 and Figure 2 present the performance of graph domain adaptations, with F1 scores for multi-label cases and accuracy scores for single-label cases. Δ_{Mean} in the tables indicates how a model’s performance compares to the mean performance across all models. For the *multi-step shifting* datasets, Table 3 shows the case where only the graph from the last step of shift generation is used as the target, while Figure 2 shows the case where graphs from each step of shift generation are treated as target graphs with different discrepancies from the source graph.

As shown in the tables, our proposed GGDA framework consistently outperforms other baselines given the intermediate domain construction that aims to minimize information loss upon adaptations and flexibly handles transfer scenarios with varied discrepancies. Moreover, the constructed domains effectively simulate the underlying data flow that bridges the gap, as evidenced by the small difference in target accuracy between our GGDA framework and GGDA-GT, which uses the actual intermediate data from the multi-step shifting process. Meanwhile, Figure 2 illustrates that GGDA-GCN and GGDA-GAT are the least susceptible to an increasing source-target discrepancy, and the high vulnerability of DIR-based models suggests that enforcing an alignment on domain distributions can lead to information distortion

and backfire when the domain discrepancy is large. Such a limitation of DIR has also been theoretically validated in previous studies [82].

Table 2. Micro-F1 and macro-F1 scores (i.e., F1MI and F1MA) of node classifications on the target graph.

	A to C		A to D		C to A		C to D		D to A		D to C		Δ_{Mean}
	F1MI	F1MA											
CDAN	77.4±0.3	74.7±0.5	69.6±0.5	65.3±1.5	73.7±0.3	72.5±0.5	73.9±0.3	70.9±0.6	69.0±0.4	66.3±0.7	74.3±0.3	70.8±0.6	+0.3
MDD	76.4±0.4	72.9±0.7	67.6±0.6	61.2±1.6	74.5±0.5	73.4±0.7	73.2±0.4	70.2±0.5	69.8±0.4	66.6±0.8	74.5±0.5	70.3±0.9	-0.4
UDA-GCN	74.0±0.7	71.2±1.5	69.0±0.8	61.3±2.4	72.6±0.5	71.4±0.6	71.5±0.6	66.0±2.7	70.4±0.7	67.7±2.3	74.5±0.4	71.0±1.1	-1.2
ACDNE	78.9±0.3	77.3±0.3	72.2±0.3	69.9±0.3	76.3±0.1	74.6±0.1	74.3±0.3	72.9±0.3	71.6±0.4	70.5±0.4	79.2±0.2	77.1±0.3	+3.3
ASN	78.6±0.7	73.6±1.9	72.7±1.1	66.7±2.8	72.8±0.8	72.7±1.4	74.5±0.7	72.0±1.2	69.0±1.2	68.5±3.0	78.1±0.3	74.1±1.2	+1.5
GRADE	70.8±0.6	68.4±0.8	66.4±0.4	61.6±2.1	67.9±0.3	66.3±0.4	69.6±0.5	66.3±1.0	65.0±0.7	62.1±1.0	68.3±0.5	65.2±1.2	-4.8
StruRW	65.1±2.4	63.2±1.8	68.0±2.1	62.4±2.4	70.6±2.4	66.3±2.4	71.8±2.0	70.4±1.6	65.6±2.1	61.7±1.5	69.2±2.0	60.7±2.2	-5.0
SpecReg	67.5±1.6	64.3±2.3	66.4±1.4	61.8±2.3	68.7±1.4	65.2±3.1	71.8±1.0	65.9±2.1	65.9±1.5	58.8±3.8	67.0±1.8	58.9±1.7	-6.1
GraphAlign	73.2±1.1	70.1±1.1	67.5±1.4	64.6±1.2	67.2±1.1	66.6±1.1	71.6±1.1	68.2±1.8	59.6±1.6	58.8±1.0	66.0±0.8	62.9±1.7	-4.9
A2GNN	75.5±0.3	77.4±0.3	62.1±0.4	66.3±0.3	76.3±0.2	74.9±0.1	70.5±0.4	73.5±0.3	71.7±0.3	71.5±0.2	76.5±0.2	77.8±0.1	+1.6
Pair-Align	72.4±0.6	68.3±0.6	67.5±0.5	64.3±0.3	71.2±0.7	68.5±0.3	71.3±0.3	70.4±0.2	66.1±0.4	62.9±0.6	72.4±0.5	67.2±0.4	-2.7
TDSS	79.6±0.6	77.4±0.9	74.1±0.5	69.7±0.5	74.3±0.2	75.3±0.3	75.2±0.3	73.2±0.6	71.3±0.8	71.6±0.7	80.2±0.6	77.4±0.9	+3.7
GGDA-GCN	80.3±0.3	78.8±0.2	74.7±0.3	72.2±0.3	76.0±0.1	75.9±0.2	75.7±0.5	74.3±0.5	73.7±0.3	73.2±0.3	81.6±0.3	80.7±0.2	+5.2
GGDA-GAT	81.9±0.2	80.4±0.2	77.2±0.2	74.9±0.4	77.1±0.2	76.6±0.2	77.4±0.3	75.9±0.4	75.8±0.3	75.8±0.3	81.5±0.2	80.3±0.2	+6.6
GGDA-SAGE	78.0±0.3	76.8±0.3	72.4±0.6	70.0±0.5	75.6±0.2	75.6±0.3	74.1±0.5	72.3±0.7	70.8±0.3	71.3±0.4	76.3±0.5	76.0±0.5	+2.8
Oracle	97.3±0.1	96.9±0.1	96.9±0.1	96.8±0.1	97.0±0.1	97.0±0.1	96.9±0.1	96.8±0.1	97.0±0.1	97.0±0.1	97.3±0.1	96.9±0.1	

Table 3. Node classification accuracy on the target graph. OOM indicates out-of-memory errors.

	Arxiv 2007 to					To the last step of shift generation					Δ_{Mean}	
	A2 to D2	D2 to A2	B1 to B2	B2 to B1	Arxiv 2016	Arxiv 2018	Cora	CiteSeer	ENGB	DE		PTBR
CDAN	75.8±1.8	67.5±0.6	48.0±1.0	45.7±0.9	47.4±0.1	42.6±0.4	70.2±4.2	67.8±3.6	68.6±1.9	70.7±1.8	66.5±2.3	+1.1
MDD	74.2±1.5	69.8±1.3	44.0±0.7	43.5±0.8	52.8±0.5	51.3±1.3	59.2±1.7	64.1±3.2	65.6±4.2	67.9±2.2	65.9±0.4	-0.1
UDA-GCN	79.1±2.1	71.5±1.0	43.6±1.8	45.8±2.5	54.1±0.2	53.5±0.6	56.5±3.6	71.4±4.5	62.2±3.4	69.2±2.8	71.6±2.6	+1.8
ACDNE	70.1±1.4	60.3±1.5	53.1±1.3	51.3±1.3	43.5±0.6	40.9±1.3	60.4±3.9	53.6±3.1	50.8±2.7	56.8±2.6	68.1±2.2	-4.5
ASN	85.2±1.2	64.9±1.4	30.1±1.3	38.2±2.3	OOM	OOM	78.8±1.9	70.9±3.0	56.5±1.0	59.6±2.8	67.7±2.7	+1.4
GRADE	61.1±1.9	64.4±2.4	42.5±1.3	41.4±1.0	46.8±0.4	OOM	57.9±3.2	66.5±2.5	58.1±2.8	61.2±3.3	63.4±3.3	-3.6
StruRW	63.7±2.8	66.6±2.7	38.7±2.6	31.9±1.3	31.7±0.7	27.2±0.7	67.6±1.9	62.1±4.3	55.6±2.5	60.8±2.4	61.7±2.5	-8.3
SpecReg	75.6±6.9	68.0±2.0	44.7±1.0	43.7±1.0	53.2±0.5	47.6±1.9	72.0±4.3	75.6±3.7	68.1±3.6	69.7±1.4	69.5±1.2	+2.6
GraphAlign	67.8±1.4	68.0±1.6	45.1±1.2	45.9±0.4	30.1±0.3	27.5±0.7	61.0±2.4	56.2±5.2	69.4±3.8	69.9±4.8	67.8±2.0	-4.6
A2GNN	76.1±0.1	67.9±0.7	37.2±1.6	39.5±1.2	48.4±1.1	40.1±2.6	79.7±1.9	70.4±1.7	67.7±2.2	67.1±2.1	68.9±1.7	+0.4
Pair-Align	63.3±0.4	65.7±0.4	39.1±0.7	34.0±0.6	39.2±0.4	37.2±0.7	60.7±1.4	71.4±2.7	61.5±2.0	60.4±1.3	67.9±1.9	-5.3
TDSS	72.5±0.7	64.2±0.7	34.1±1.1	32.9±0.8	43.3±0.4	OOM	79.7±1.4	70.5±2.2	62.3±1.3	62.0±1.4	69.1±1.5	-0.9
GGDA-GCN	91.5±0.5	70.0±0.8	52.4±1.7	49.3±0.4	56.8±0.5	56.6±0.5	86.6±2.1	74.1±3.4	75.3±0.6	74.6±0.4	72.2±0.8	+9.1
GGDA-GAT	91.5±0.4	70.3±0.5	31.5±0.6	30.9±0.9	54.7±0.4	54.1±0.5	82.6±2.2	82.7±1.1	74.2±1.6	74.5±1.7	76.9±1.5	+5.9
GGDA-SAGE	78.5±0.6	58.2±0.5	50.2±1.0	50.3±1.0	55.0±0.1	53.2±0.4	87.4±1.2	83.6±1.1	61.8±1.2	64.8±1.0	70.5±0.9	+4.0
GGDA-GT	/	/	/	/	/	/	93.8±0.2	88.5±0.2	77.7±0.4	74.8±0.7	77.3±0.3	
Oracle	92.4±0.1	99.2±0.1	71.4±2.2	72.3±0.9	67.5±0.1	67.9±0.1	99.0±0.2	95.0±0.2	81.1±0.4	77.6±0.4	78.0±0.4	

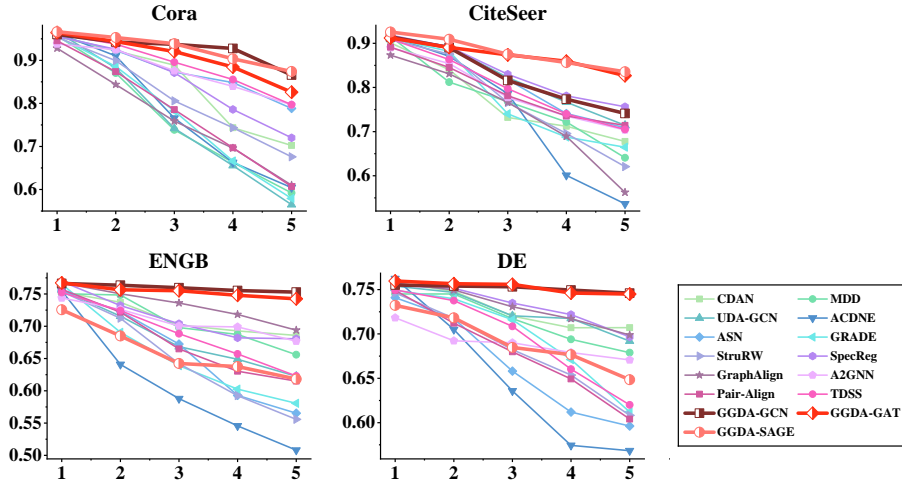


Fig. 2. Node classification accuracy on target graphs with varying levels of discrepancy from the source graph. The x-axis shows the source-target discrepancy level ranked from 1 (closest) to 5 (farthest). The y-axis shows the classification accuracy.

Table 4. Performance drop in target graph node classifications across variants compared to the complete GGDA framework.

	A to D	D to C	C to A	A2 to D2	B1 to B2	Arxiv(07-16)	Arxiv(07-18)	CiteSeer	DE	PTBR	Avg. Drop
Source	-10.7±0.7	-11.0±0.9	-6.0±0.2	-17.0±0.9	-15.1±1.7	-5.6±0.9	-7.8±0.9	-15.8±4.9	-34.9±0.6	-37.2±1.1	-16.1
Direct ST	-6.7±0.6	-5.0±0.5	-3.2±0.3	-11.8±1.2	-11.2±2.4	-5.1±0.8	-7.6±1.1	-7.9±5.0	-7.3±6.4	-22.7±2.9	-8.9
DIR	-9.6±1.3	-13.1±1.2	-8.9±0.8	-11.1±3.5	-4.3±3.4	-4.3±1.0	-4.1±1.1	-21.2±6.5	-3.1±3.8	-6.6±1.4	-8.6
GGDA-I	-2.5±0.7	-5.2±0.6	-1.5±0.4	-7.5±2.6	-10.2±3.1	-2.1±1.0	-2.9±1.1	-4.1±7.1	-6.1±3.7	-4.7±4.1	-4.7
GGDA-R	-2.7±0.7	-1.3±0.7	-1.7±0.6	-0.7±0.6	-3.8±2.1	-2.0±0.5	-2.0±0.9	-2.0±5.9	-0.7±0.7	-1.5±1.0	-1.9

10.4 Ablation Studies

To investigate the effectiveness of different components, we conduct ablation studies as follows. (1) **Source**: direct transfer with a classifier trained on source; (2) **Direct ST**: self-training (i.e., iterative pseudo-labeling) without intermediate samples; (3) **DIR**: a prevalent graph DA framework with an adversarial domain classifier for distribution alignment; (4) **GGDA-I (Isolated)**: GGDA with each isolated graph $\tilde{\mu}_k$ as a separate domain; (5) **GGDA-R (Random)**: GGDA with a random matching function $m(\cdot)$ for graph generation. We adopt GCN in all cases, with the results shown in Table 4. Particularly, the significant performance drop of Direct ST and DIR highlights the crucial role of intermediate domains in exploiting the underlying data patterns for a robust graph DA. Meanwhile, DIR shows signs of negative transfer (i.e., lower accuracy than Source), underscoring the instability of domain alignment and its heavy reliance on additional model designs. The performance drop of GGDA-I validates the effectiveness of our dual modules in enhancing GGDA via the bonding of knowledge-preserving vertices and adaptive domain advancement, while the performance drop of GGDA-R reflects the improved information integrity from entropy-guided matching in graph generation.

10.5 Hyperparameter Analysis

The effects of κ and β are shown in Figure 3 and 4. From Figure 3, we observe that adjusting κ enables flexible domain constructions under varying inter-domain distance $W_p(\mu_t, \mu_{t+1})$ while maintaining an inverse relationship between the average distance Δ and the number of domains T . Meanwhile, Figure 4 shows that the optimal GGDA domain path occurs at a "sweet spot" when κ , and thus T , is not too small or too large, which aligns with the initial theoretical analysis. As for β , which governs the pace of weight decay, setting it to 0 equates to self-training on the entire graph sequence without considering distribution shifts, while an overly large β causes rapid information decay before full utilization, both of which can deteriorate transfer performance.

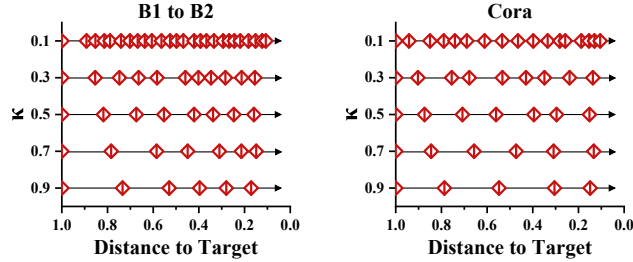


Fig. 3. Progression of the constructed domain sequence under different κ . The x-axis shows the normalized embedding distance between the current and target domains.

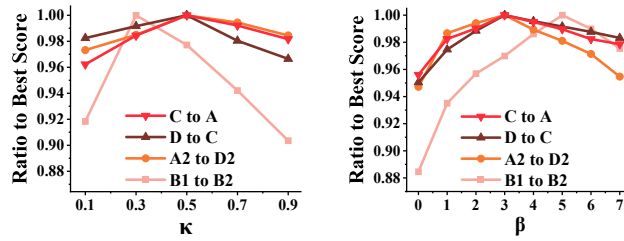


Fig. 4. Performance of our GGDA framework with varying values of hyperparameters κ and β .

10.6 Visualization of Adaptive Mass Decay

Figure 5 demonstrates the effect of mass decay across GGDA stages. For a clearer interpretation, here we omit the operation that zeroes out lower-ranked weights in domain constructions. We observe a progressive fading of color from top to bottom and from right to left, indicating that the importance of past domains undergoes a cumulative decay as the model advances, and in each stage, the domain distribution shifts towards new dominant nodes. We also observe that consecutive vertex sets could carry higher weights in later stages. This is because the normalized η -penalty could slightly slow down the domain shift when approaching the target domain, resulting in more overlap between adjacent vertex sets. Notably, the bottom-left grid can be interpreted as the proportion of source samples that explicitly share common ego-graph properties with the final domain.

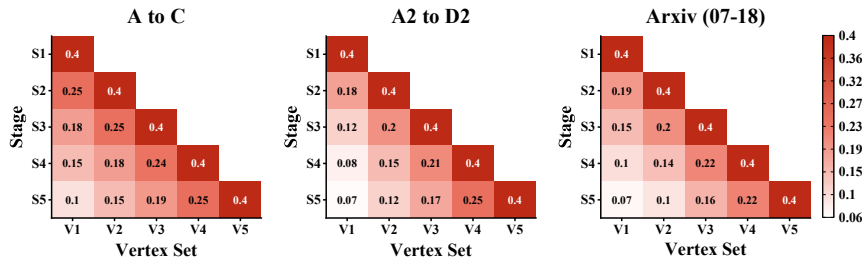


Fig. 5. Visualization of mass decay in each stage of GGDA. The x-axis represents the set of the top-weighted vertices constituting 40% of each domain distribution, and the y-axis represents the stage of GGDA. The color of the squares indicates the sum of weights over each vertex set in each stage.

10.7 Visualization of Target Representation Space

Figure 6 illustrates the final target representation space given by the symbolic DIR model, UDA-GCN, and our proposed GGDA framework. Specifically, we project the node embeddings onto a two-dimensional space via the t-SNE algorithm [60]. In the visualizations, the node embeddings produced by UDA-GCN exhibit greater overlap and mixing between different classes, while the ones generated by GGDA demonstrate a well-separated clustering with more pronounced class boundaries. The improved ability of GGDA to learn class-discriminative target representations is attributed to its careful domain sequence constructions that aim for the optimal adaptation path to minimize information loss and reduce irrelevant noise. The preservation of transferable information from the labeled source graph allows GGDA to achieve stable transfer under arbitrary source-target discrepancies.

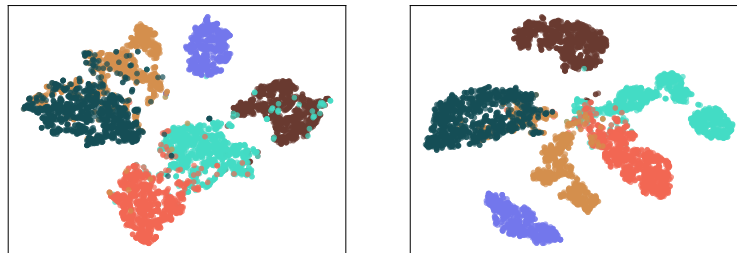


Fig. 6. Visualization of target graph node embeddings for the task A2 to D2, where distinct colors signify different class labels. The left side shows the result from UDA-GCN and the right side shows that from GGDA-GCN.

10.8 Visualization of Knowledge Transfer in GGDA

To delve into the process of knowledge transfer in GGDA, we conduct an experiment on a synthetic dataset generated using contextual stochastic block model (CSBM) [11], where node attributes and edges are generated independently given node labels. Specifically, we construct the source and target graphs to each contain 300 nodes, with 100 nodes from each of the 3 classes. We generate the node attributes for the three classes with Gaussians $\mathbb{P}_0 = \mathcal{N}([0, -3], I/2)$, $\mathbb{P}_1 = \mathcal{N}([0, 0], I/2)$, and $\mathbb{P}_2 = \mathcal{N}([0, 3], I/2)$ for the source graph, and Gaussians $\mathbb{P}_0 = \mathcal{N}([6, -3], I/2)$, $\mathbb{P}_1 = \mathcal{N}([6, 0], I/2)$, and $\mathbb{P}_2 = \mathcal{N}([6, 3], I/2)$ for the target graph. In both graphs, the intra-class edge probability is set to 0.1, while the inter-class edge probability is set to 0.02. To widen the distribution gap, we further modify the target graph by replacing

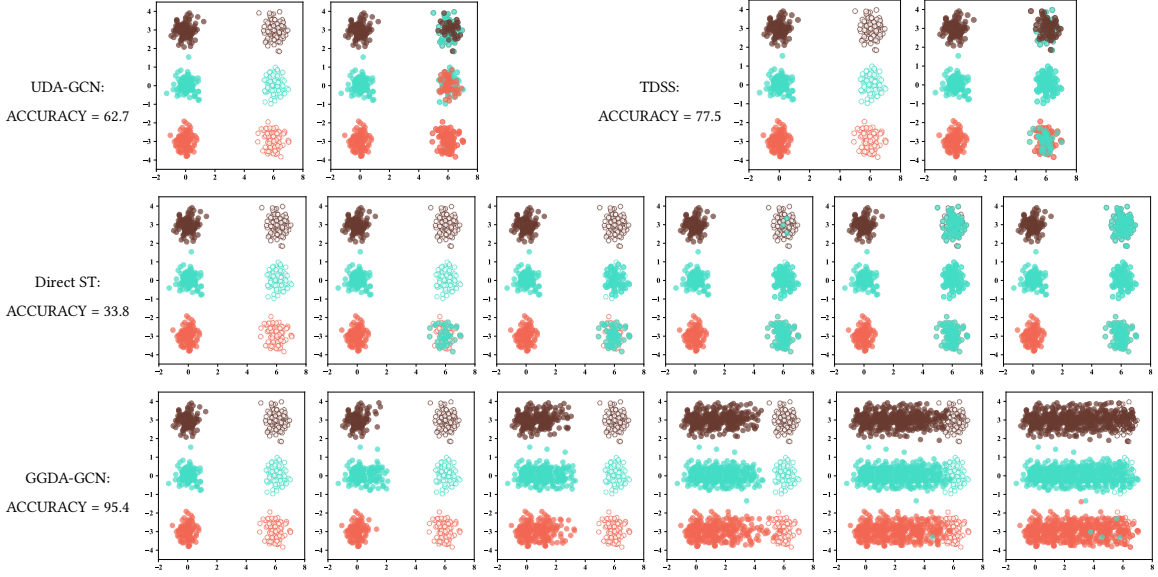


Fig. 7. Each plane represents a 2-dimensional space Ω_x (note that all computations are performed over the product space $\Omega_x \times \Omega_a$, i.e., with both features and structures on graph (non-IID), but the visualization is shown on Ω_x for clarity). Solid circles represent the ground-truth source labels or the assigned pseudo-labels (i.e., predictions) on each sample, whereas hollow circles represent the ground-truth target labels. Distinct colors indicate different classes. The assignments of labels throughout the training process are shown from left to right, with the leftmost planes showing the source and target labels before training. Specifically, UDA-GCN and TDSS employ single-stage training, while Direct ST and GGDA-GCN employ multi-stage training.

25% of the randomly generated intra-class edges with intra-class edges that connect the top-k dissimilar nodes based on their attributes.

Figure 7 demonstrates knowledge transfer in UDA-GCN, TDSS, Direct ST, and GGDA-GCN via the label assignments from training. While visualized in Ω_x for clarity, we emphasize that the actual computations operate over $\Omega_x \times \Omega_a$ with interactions between node features and local graph structures — where the key complexity arises. The figure reveals that, through careful graph generation and iterative domain construction strategy, GGDA effectively creates an optimal domain path over the manifold. It regularizes transfer errors over consecutive domains, thus overcoming the significant distribution gap with minimal noise disturbance to allow smooth and accurate transition to the target graph.

Knowledge distortion occurs with methods other than GGDA-GCN. For DIR models (i.e., UDA-GCN and TDSS), domain alignment forcibly matches the overall distributions while neglecting source-target correlations in the joint space, rendering them unreliable under a widened distribution gap. As for Direct ST, pseudo-labels are initially assigned to target nodes solely based on the source model, but with large domain discrepancies, many become inaccurate. The erroneous information propagates upon the target graph during subsequent training stages, impeding proper learning.

10.9 Runtime Comparison

Table 5 compares the model efficiency on transfer Arxiv(07-18), the largest dataset. All models are trained until convergence at either around 1000 or 200 epochs. Our GGDA framework achieves a runtime comparable to other models while significantly improving target predictions. Despite the non-generative nature of DIR models, they rely heavily

Table 5. Comparison of runtime on Arxiv(07-18) (for 1000 epochs) and average performance score across all datasets.

Model	Runtime (seconds)	Avg. Score
SpecReg	532.3	63.9
A2GNN	643.6	66.8
ACDNE	1849.9 (for 200 epochs)	65.4
GraphAlign	1422.7 (for 200 epochs)	61.1
GGDA-GCN	668.2 (graph generation) + 208.5 (domain progression) = 876.7	72.9

on advanced encoder designs and regularizations, leading to costly computations such as eigendecomposition and topological matching. As for GraphAlign, a data-centric method, the graph generation is computationally intensive when the generated graph exceeds 1% of the target graph size, i.e., a huge trade-off between time and performance. Overall, our novel GGDA framework strikes an optimal balance via the accelerated graph generation technique and the careful domain constructions that attain minimal transfer information loss.

11 CONCLUSION

This work presents a pioneering effort to tackle the significant challenge of large inter-graph distribution shifts by establishing a novel graph gradual domain adaptation (GGDA) framework. Moving beyond the limitations of traditional domain-invariant methods and existing IID-focused gradual adaptation techniques, GGDA is specifically engineered for the complexities of non-IID graph-structured data.

Our solution is built on two foundational pillars. First, we introduce an efficient method for generating a knowledge-preserving intermediate data bridge by computing the weighted Fréchet mean over the Fused Gromov-Wasserstein (FGW) metric. This allows us to bypass the inherent implicitness of cross-domain graph structure space and generate intermediate graphs that faithfully integrate node features and structural relations from source and target graphs. Second, upon this bridge, we develop a novel vertex-based domain progression scheme. This scheme constructs an optimal adaptation path by strategically selecting "close" vertices and adaptively advancing the domain, thereby ensuring minimal information loss and maximizing the preservation of transferable, discriminative knowledge throughout the GGDA domain sequence.

Theoretical analysis forms a critical component of our contribution. We demonstrate that our framework concretizes $W_p(\mu_t, \mu_{t+1})$, the otherwise intractable inter-domain Wasserstein distance over the graph space $\Omega_x \times \Omega_a \times \Omega_y$, by establishing implementable lower and upper bounds for it. The lower bound is derived from the FGW metric, while the upper bound is governed by our vertex selection regularization. This theoretical grounding not only provides a rigorous justification for our approach but also offers a flexible mechanism – via a simple hyperparameter – to adjust the inter-domain compactness and optimize the entire domain sequence without costly regenerations.

Extensive experiments validate the superiority of GGDA over state-of-the-art methods across diverse transfer scenarios. Looking forward, the GGDA framework opens up promising avenues for future research and could be extended to other complex non-IID learning scenarios, such as hypergraphs, dynamic graphs, and knowledge graphs.

ACKNOWLEDGMENTS

This work was supported by the Science and Technology Development Fund (FDCT) [grant number 0126/2024/RIA2].

REFERENCES

- [1] Samira Abnar, Rianne van den Berg, Golnaz Ghiasi, Mostafa Dehghani, Nal Kalchbrenner, and Hanie Sedghi. 2021. Gradual domain adaptation in the wild: When intermediate distributions are absent. *arXiv preprint arXiv:2106.06080* (2021).
- [2] Konstantinos Bousmalis, George Trigeorgis, Nathan Silberman, Dilip Krishnan, and Dumitru Erhan. 2016. Domain separation networks. *Advances in neural information processing systems* 29 (2016).
- [3] Ruichu Cai, Fengzhu Wu, Zijian Li, Pengfei Wei, Lingling Yi, and Kun Zhang. 2024. Graph domain adaptation: A generative view. *ACM Transactions on Knowledge Discovery from Data* 18, 3 (2024), 1–24.
- [4] Benson Chen, Gary Bécigneul, Octavian-Eugen Ganea, Regina Barzilay, and Tommi Jaakkola. 2020. Optimal transport graph neural networks. *arXiv preprint arXiv:2006.04804* (2020).
- [5] Hong-You Chen and Wei-Lun Chao. 2021. Gradual domain adaptation without indexed intermediate domains. *Advances in neural information processing systems* 34 (2021), 8201–8214.
- [6] Wei Chen, Guo Ye, Yakun Wang, Zhao Zhang, Libang Zhang, Daixin Wang, Zhiqiang Zhang, and Fuzhen Zhuang. 2025. Smoothness Really Matters: A Simple Yet Effective Approach for Unsupervised Graph Domain Adaptation. In *Proceedings of the AAAI Conference on Artificial Intelligence*, Vol. 39. 15875–15883.
- [7] Samir Chowdhury and Tom Needham. 2021. Generalized spectral clustering via Gromov-Wasserstein learning. In *International Conference on Artificial Intelligence and Statistics*. PMLR, 712–720.
- [8] Nicolas Courty, Rémi Flamary, Devis Tuia, and Alain Rakotomamonjy. 2016. Optimal transport for domain adaptation. *IEEE transactions on pattern analysis and machine intelligence* 39, 9 (2016), 1853–1865.
- [9] Quanyu Dai, Xiao-Ming Wu, Jiaren Xiao, Xiao Shen, and Dan Wang. 2022. Graph transfer learning via adversarial domain adaptation with graph convolution. *IEEE Transactions on Knowledge and Data Engineering* 35, 5 (2022), 4908–4922.
- [10] Michaël Defferrard, Xavier Bresson, and Pierre Vandergheynst. 2016. Convolutional neural networks on graphs with fast localized spectral filtering. *Advances in neural information processing systems* 29 (2016).
- [11] Yash Deshpande, Subhabrata Sen, Andrea Montanari, and Elchanan Mossel. 2018. Contextual stochastic block models. *Advances in Neural Information Processing Systems* 31 (2018).
- [12] Cornelia Druţu and Michael Kapovich. 2018. *Geometric group theory*. Vol. 63. American Mathematical Soc.
- [13] Yaroslav Ganin, Evgeniya Ustinova, Hana Ajakan, Pascal Germain, Hugo Larochelle, François Laviolette, Mario March, and Victor Lempitsky. 2016. Domain-adversarial training of neural networks. *Journal of machine learning research* 17, 59 (2016), 1–35.
- [14] Vikas Garg, Stefanie Jegelka, and Tommi Jaakkola. 2020. Generalization and representational limits of graph neural networks. In *International Conference on Machine Learning*. PMLR, 3419–3430.
- [15] Justin Gilmer, Samuel S Schoenholz, Patrick F Riley, Oriol Vinyals, and George E Dahl. 2017. Neural message passing for quantum chemistry. In *International conference on machine learning*. PMLR, 1263–1272.
- [16] Boqing Gong, Yuan Shi, Fei Sha, and Kristen Grauman. 2012. Geodesic flow kernel for unsupervised domain adaptation. In *2012 IEEE conference on computer vision and pattern recognition*. IEEE, 2066–2073.
- [17] Rui Gong, Wen Li, Yuhua Chen, and Luc Van Gool. 2019. Dlow: Domain flow for adaptation and generalization. In *Proceedings of the IEEE/CVF conference on computer vision and pattern recognition*. 2477–2486.
- [18] Raghuraman Gopalan, Ruonan Li, and Rama Chellappa. 2011. Domain adaptation for object recognition: An unsupervised approach. In *2011 international conference on computer vision*. IEEE, 999–1006.
- [19] Gaoyang Guo, Chaokun Wang, Bencheng Yan, Yunkai Lou, Hao Feng, Junchao Zhu, Jun Chen, Fei He, and S Yu Philip. 2022. Learning adaptive node embeddings across graphs. *IEEE Transactions on Knowledge and Data Engineering* 35, 6 (2022), 6028–6042.
- [20] Will Hamilton, Zitao Ying, and Jure Leskovec. 2017. Inductive representation learning on large graphs. *Advances in neural information processing systems* 30 (2017).
- [21] Yifei He, Haoxiang Wang, Bo Li, and Han Zhao. 2023. Gradual Domain Adaptation: Theory and Algorithms. *arXiv preprint arXiv:2310.13852* (2023).
- [22] Han-Kai Hsu, Chun-Han Yao, Yi-Hsuan Tsai, Wei-Chih Hung, Hung-Yu Tseng, Maneesh Singh, and Ming-Hsuan Yang. 2020. Progressive domain adaptation for object detection. In *Proceedings of the IEEE/CVF winter conference on applications of computer vision*. 749–757.
- [23] Weihua Hu, Matthias Fey, Marinka Zitnik, Yuxiao Dong, Hongyu Ren, Bowen Liu, Michele Catasta, and Jure Leskovec. 2020. Open graph benchmark: Datasets for machine learning on graphs. *Advances in neural information processing systems* 33 (2020), 22118–22133.
- [24] Renhong Huang, Jiarong Xu, Xin Jiang, Ruichuan An, and Yang Yang. 2024. Can Modifying Data Address Graph Domain Adaptation?. In *Proceedings of the 30th ACM SIGKDD Conference on Knowledge Discovery and Data Mining*. 1131–1142.
- [25] Leonid V Kantorovich. 1960. Mathematical methods of organizing and planning production. *Management science* 6, 4 (1960), 366–422.
- [26] George Karypis and Vipin Kumar. 1998. A fast and high quality multilevel scheme for partitioning irregular graphs. *SIAM Journal on scientific Computing* 20, 1 (1998), 359–392.
- [27] Thomas N Kipf and Max Welling. 2016. Semi-supervised classification with graph convolutional networks. *arXiv preprint arXiv:1609.02907* (2016).
- [28] Ananya Kumar, Tengyu Ma, and Percy Liang. 2020. Understanding self-training for gradual domain adaptation. In *International conference on machine learning*. PMLR, 5468–5479.

- [29] Jundong Li, Xia Hu, Jiliang Tang, and Huan Liu. 2015. Unsupervised streaming feature selection in social media. In *Proceedings of the 24th ACM International on Conference on Information and Knowledge Management*. 1041–1050.
- [30] Jiajin Li, Jianheng Tang, Leming Kong, Huikang Liu, Jia Li, Anthony Man-Cho So, and Jose Blanchet. 2023. A convergent single-loop algorithm for relaxation of gromov-wasserstein in graph data. *arXiv preprint arXiv:2303.06595* (2023).
- [31] Meihan Liu, Zeyu Fang, Zhen Zhang, Ming Gu, Sheng Zhou, Xin Wang, and Jiajun Bu. 2024. Rethinking Propagation for Unsupervised Graph Domain Adaptation. *arXiv preprint arXiv:2402.05660* (2024).
- [32] Ming-Yu Liu and Oncel Tuzel. 2016. Coupled generative adversarial networks. *Advances in neural information processing systems* 29 (2016).
- [33] Shikun Liu, Tianchun Li, Yongbin Feng, Nhan Tran, Han Zhao, Qiang Qiu, and Pan Li. 2023. Structural re-weighting improves graph domain adaptation. In *International Conference on Machine Learning*. PMLR, 21778–21793.
- [34] Shikun Liu, Deyu Zou, Han Zhao, and Pan Li. 2024. Pairwise Alignment Improves Graph Domain Adaptation. *arXiv preprint arXiv:2403.01092* (2024).
- [35] Mingsheng Long, Zhangjie Cao, Jianmin Wang, and Michael I Jordan. 2018. Conditional adversarial domain adaptation. *Advances in neural information processing systems* 31 (2018).
- [36] Mingsheng Long, Han Zhu, Jianmin Wang, and Michael I Jordan. 2017. Deep transfer learning with joint adaptation networks. In *International conference on machine learning*. PMLR, 2208–2217.
- [37] Xinyu Ma, Xu Chu, Yasha Wang, Yang Lin, Junfeng Zhao, Liantao Ma, and Wenwu Zhu. 2024. Fused Gromov-Wasserstein Graph Mixup for Graph-level Classifications. *Advances in Neural Information Processing Systems* 36 (2024).
- [38] Yuzhen Mao, Jianhui Sun, and Dawei Zhou. 2022. Augmenting Knowledge Transfer across Graphs. In *2022 IEEE International Conference on Data Mining (ICDM)*. IEEE, 1101–1106.
- [39] Facundo Mémoli. 2011. Gromov-Wasserstein distances and the metric approach to object matching. *Foundations of computational mathematics* 11 (2011), 417–487.
- [40] Jaemin Na, Heechul Jung, Hyung Jin Chang, and Wonjun Hwang. 2021. Fixbi: Bridging domain spaces for unsupervised domain adaptation. In *Proceedings of the IEEE/CVF conference on computer vision and pattern recognition*. 1094–1103.
- [41] Sinno Jialin Pan and Qiang Yang. 2009. A survey on transfer learning. *IEEE Transactions on knowledge and data engineering* 22, 10 (2009), 1345–1359.
- [42] Gabriel Peyré, Marco Cuturi, et al. 2019. Computational optimal transport: With applications to data science. *Foundations and Trends® in Machine Learning* 11, 5-6 (2019), 355–607.
- [43] Gabriel Peyré, Marco Cuturi, and Justin Solomon. 2016. Gromov-wasserstein averaging of kernel and distance matrices. In *International conference on machine learning*. PMLR, 2664–2672.
- [44] Ziyue Qiao, Xiao Luo, Meng Xiao, Hao Dong, Yuanchun Zhou, and Hui Xiong. 2023. Semi-supervised domain adaptation in graph transfer learning. *arXiv preprint arXiv:2309.10773* (2023).
- [45] Benedek Rozemberczki, Carl Allen, and Rik Sarkar. 2021. Multi-scale attributed node embedding. *Journal of Complex Networks* 9, 2 (2021), cnab014.
- [46] Yossi Rubner, Carlo Tomasi, and Leonidas J Guibas. 2000. The earth mover’s distance as a metric for image retrieval. *International journal of computer vision* 40 (2000), 99–121.
- [47] Shogo Sagawa and Hideitsu Hino. 2022. Gradual domain adaptation via normalizing flows. *arXiv preprint arXiv:2206.11492* (2022).
- [48] Meyer Scetbon, Gabriel Peyré, and Marco Cuturi. 2022. Linear-time gromov wasserstein distances using low rank couplings and costs. In *International Conference on Machine Learning*. PMLR, 19347–19365.
- [49] Prithviraj Sen, Galileo Namata, Mustafa Bilgic, Lise Getoor, Brian Galligher, and Tina Eliassi-Rad. 2008. Collective classification in network data. *AI magazine* 29, 3 (2008), 93–93.
- [50] Kendrick Shen, Robbie M Jones, Ananya Kumar, Sang Michael Xie, Jeff Z HaoChen, Tengyu Ma, and Percy Liang. 2022. Connect, not collapse: Explaining contrastive learning for unsupervised domain adaptation. In *International conference on machine learning*. PMLR, 19847–19878.
- [51] Xiao Shen, Quanyu Dai, Fu-lai Chung, Wei Lu, and Kup-Sze Choi. 2020. Adversarial deep network embedding for cross-network node classification. In *Proceedings of the AAAI conference on artificial intelligence*, Vol. 34. 2991–2999.
- [52] Boshen Shi, Yongqing Wang, Fangda Guo, Jiangli Shao, Huawei Shen, and Xueqi Cheng. 2023. Improving graph domain adaptation with network hierarchy. In *Proceedings of the 32nd ACM International Conference on Information and Knowledge Management*. 2249–2258.
- [53] Lianghe Shi and Weiwei Liu. 2024. Adversarial Self-Training Improves Robustness and Generalization for Gradual Domain Adaptation. *Advances in Neural Information Processing Systems* 36 (2024).
- [54] Hidetoshi Shimodaira. 2000. Improving predictive inference under covariate shift by weighting the log-likelihood function. *Journal of statistical planning and inference* 90, 2 (2000), 227–244.
- [55] Ankit Singh. 2021. Clda: Contrastive learning for semi-supervised domain adaptation. *Advances in Neural Information Processing Systems* 34 (2021), 5089–5101.
- [56] Ben Tan, Yangqiu Song, Erheng Zhong, and Qiang Yang. 2015. Transitive transfer learning. In *Proceedings of the 21th ACM SIGKDD international conference on knowledge discovery and data mining*. 1155–1164.
- [57] Ben Tan, Yu Zhang, Sinno Pan, and Qiang Yang. 2017. Distant domain transfer learning. In *Proceedings of the AAAI conference on artificial intelligence*, Vol. 31.
- [58] Vayer Titouan, Nicolas Courty, Romain Tavenard, and Rémi Flamary. 2019. Optimal transport for structured data with application on graphs. In *International Conference on Machine Learning*. PMLR, 6275–6284.

- [59] Eric Tzeng, Judy Hoffman, Kate Saenko, and Trevor Darrell. 2017. Adversarial discriminative domain adaptation. In *Proceedings of the IEEE conference on computer vision and pattern recognition*. 7167–7176.
- [60] Laurens Van der Maaten and Geoffrey Hinton. 2008. Visualizing data using t-SNE. *Journal of machine learning research* 9, 11 (2008).
- [61] Titouan Vayer, Laetitia Chapel, Rémi Flamary, Romain Tavenard, and Nicolas Courty. 2020. Fused Gromov-Wasserstein distance for structured objects. *Algorithms* 13, 9 (2020), 212.
- [62] Petar Veličković, Guillem Cucurull, Arantxa Casanova, Adriana Romero, Pietro Lio, and Yoshua Bengio. 2017. Graph attention networks. *arXiv preprint arXiv:1710.10903* (2017).
- [63] Cédric Vincent-Cuaz, Rémi Flamary, Marco Corneli, Titouan Vayer, and Nicolas Courty. 2021. Semi-relaxed Gromov-Wasserstein divergence with applications on graphs. *arXiv preprint arXiv:2110.02753* (2021).
- [64] Cédric Vincent-Cuaz, Rémi Flamary, Marco Corneli, Titouan Vayer, and Nicolas Courty. 2022. Template based graph neural network with optimal transport distances. *Advances in Neural Information Processing Systems* 35 (2022), 11800–11814.
- [65] Cédric Vincent-Cuaz, Titouan Vayer, Rémi Flamary, Marco Corneli, and Nicolas Courty. 2021. Online graph dictionary learning. In *International conference on machine learning*. PMLR, 10564–10574.
- [66] Haoxiang Wang, Bo Li, and Han Zhao. 2022. Understanding gradual domain adaptation: Improved analysis, optimal path and beyond. In *International Conference on Machine Learning*. PMLR, 22784–22801.
- [67] Yu Wang, Ronghang Zhu, Pengsheng Ji, and Sheng Li. 2024. Open-Set Graph Domain Adaptation via Separate Domain Alignment. In *Proceedings of the AAAI Conference on Artificial Intelligence*, Vol. 38. 9142–9150.
- [68] Jun Wu, Jingrui He, and Elizabeth Ainsworth. 2023. Non-iid transfer learning on graphs. In *Proceedings of the AAAI Conference on Artificial Intelligence*, Vol. 37. 10342–10350.
- [69] Man Wu, Shirui Pan, Chuan Zhou, Xiaojun Chang, and Xingquan Zhu. 2020. Unsupervised domain adaptive graph convolutional networks. In *Proceedings of The Web Conference 2020*. 1457–1467.
- [70] Man Wu, Shirui Pan, and Xingquan Zhu. 2022. Attraction and repulsion: Unsupervised domain adaptive graph contrastive learning network. *IEEE Transactions on Emerging Topics in Computational Intelligence* 6, 5 (2022), 1079–1091.
- [71] Yifan Wu, Ezra Winston, Divyansh Kaushik, and Zachary Lipton. 2019. Domain adaptation with asymmetrically-relaxed distribution alignment. In *International conference on machine learning*. PMLR, 6872–6881.
- [72] Hongteng Xu, Dixin Luo, and Lawrence Carin. 2019. Scalable Gromov-Wasserstein learning for graph partitioning and matching. *Advances in neural information processing systems* 32 (2019).
- [73] Hongteng Xu, Dixin Luo, Hongyuan Zha, and Lawrence Carin Duke. 2019. Gromov-wasserstein learning for graph matching and node embedding. In *International conference on machine learning*. PMLR, 6932–6941.
- [74] Keyulu Xu, Weihua Hu, Jure Leskovec, and Stefanie Jegelka. 2018. How powerful are graph neural networks? *arXiv preprint arXiv:1810.00826* (2018).
- [75] Minghao Xu, Jian Zhang, Bingbing Ni, Teng Li, Chengjie Wang, Qi Tian, and Wenjun Zhang. 2020. Adversarial domain adaptation with domain mixup. In *Proceedings of the AAAI conference on artificial intelligence*, Vol. 34. 6502–6509.
- [76] Nan Yin, Li Shen, Baopu Li, Mengzhu Wang, Xiao Luo, Chong Chen, Zhigang Luo, and Xian-Sheng Hua. 2022. Deal: An unsupervised domain adaptive framework for graph-level classification. In *Proceedings of the 30th ACM International Conference on Multimedia*. 3470–3479.
- [77] Nan Yin, Li Shen, Mengzhu Wang, Long Lan, Zeyu Ma, Chong Chen, Xian-Sheng Hua, and Xiao Luo. 2023. Coco: A coupled contrastive framework for unsupervised domain adaptive graph classification. In *International Conference on Machine Learning*. PMLR, 40040–40053.
- [78] Yuning You, Tianlong Chen, Zhangyang Wang, and Yang Shen. 2023. Graph domain adaptation via theory-grounded spectral regularization. In *The eleventh international conference on learning representations*.
- [79] Xiaowen Zhang, Yuntao Du, Rongbiao Xie, and Chongjun Wang. 2021. Adversarial separation network for cross-network node classification. In *Proceedings of the 30th ACM international conference on information & knowledge management*. 2618–2626.
- [80] Yuchen Zhang, Tianle Liu, Mingsheng Long, and Michael Jordan. 2019. Bridging theory and algorithm for domain adaptation. In *International conference on machine learning*. PMLR, 7404–7413.
- [81] Yizhou Zhang, Guojie Song, Lun Du, Shuwen Yang, and Yilun Jin. 2019. Dane: Domain adaptive network embedding. *arXiv preprint arXiv:1906.00684* (2019).
- [82] Han Zhao, Remi Tachet Des Combes, Kun Zhang, and Geoffrey Gordon. 2019. On learning invariant representations for domain adaptation. In *International conference on machine learning*. PMLR, 7523–7532.
- [83] Jun-Yan Zhu, Taesung Park, Phillip Isola, and Alexei A Efros. 2017. Unpaired image-to-image translation using cycle-consistent adversarial networks. In *Proceedings of the IEEE international conference on computer vision*. 2223–2232.
- [84] Meiqi Zhu, Xiao Wang, Chuan Shi, Houye Ji, and Peng Cui. 2021. Interpreting and unifying graph neural networks with an optimization framework. In *Proceedings of the Web Conference 2021*. 1215–1226.
- [85] Qi Zhu, Carl Yang, Yidan Xu, Haonan Wang, Chao Zhang, and Jiawei Han. 2021. Transfer learning of graph neural networks with ego-graph information maximization. *Advances in Neural Information Processing Systems* 34 (2021), 1766–1779.